© 2019. Published by The Company of Biologists Ltd | Development (2019) 146, dev181065. doi:10.1242/dev.181065

RESEARCH ARTICLE

The minimal gap-junction network among melanophores and xanthophores required for stripe pattern formation in zebrafish

Yuu Usui[1], Toshihiro Aramaki[1], Shigeru Kondo[1,2] and Masakatsu Watanabe[1,*]

ABSTRACT

Connexin 39.4 (Cx39.4) and connexin 41.8 (Cx41.8), two gap-junction proteins expressed in both melanophores and xanthophores, are crucial for the intercellular communication among pigment cells that is necessary for generating the stripe pigment pattern of zebrafish. We have previously characterized the gap-junction properties of Cx39.4 and Cx41.8, but how these proteins contribute to stripe formation remains unclear; this is because distinct types of connexins potentially form heteromeric gap junctions, which precludes accurate elucidation of individual connexin functions *in vivo*. Here, by arranging Cx39.4 and Cx41.8 expression in pigment cells, we have identified the simplest gap-junction network required for stripe generation: Cx39.4 expression in melanophores is required but expression in xanthophores is not necessary for stripe patterning, whereas Cx41.8 expression in xanthophores is sufficient for the patterning, and Cx41.8 expression in melanophores might stabilize the stripes. Moreover, patch-clamp recordings revealed that Cx39.4 gap junctions exhibit spermidine-dependent rectification property. Our results suggest that Cx39.4 facilitates the crucial cell-cell interactions between melanophores and xanthophores that mediate a unidirectional activation-signal transfer from xanthophores to melanophores, which is essential for melanophore survival.

KEY WORDS: Connexin, Gap junction, Pigment cell, Skin pattern, Zebrafish

INTRODUCTION

Gap junctions mediate direct intercellular communication involving the transfer of molecules such as <1000 Da molecules, metabolites and ions between adjacent cells (Simpson et al., 1977). Connexin is a gap-junction protein; six connexins form a hemichannel called the connexon, and the docking of opposing hemichannels between neighboring cells generates the gap junction (Fig. S1A) (Bruzzone et al., 1996; Kumar and Gilula, 1996; Saez et al., 2003). Connexin is a four-transmembrane protein, the N- and C-terminal domains of which are located in the cytoplasm (Unger et al., 1999; Willecke et al., 2002). Whereas the N terminus functions as a voltage sensor and controls the channel opening/closing machinery (Gonzalez et al., 2007; Verselis et al., 1994), the C terminus performs multiple functions and controls the assembly of connexins, the opening/closing of gap junctions, and the degradation of gap junctions by recruiting proteins such as ZO-1, actin, tubulin and protein kinases (Giepmans et al., 2001; Smyth et al., 2012; Toyofuku et al., 1998; Wang and Peracchia, 1997). In the chordate genome, connexin genes form a large family: ∼20 connexin genes have been identified in the mammalian genome (Kosakovsky Pond et al., 2007) and ∼40 connexin genes are predicted in the teleost genome (Eastman et al., 2006).

Recent studies have enhanced our understanding of bioelectric signaling in not only neuronal cells but also in organ development and regeneration (Levin, 2007; Plotkin et al., 2016). For example, loss of connexin 43 (Cx43) gap-junction function correlates with fin shortening in zebrafish (Hoptak-Solga et al., 2007), and aberrant Cx43 hemichannel activity causes a reduction of vertebral length along the anterior-posterior axis (Misu et al., 2016). Moreover, in the *Xenopus* embryo, gap-junction function is crucial for left-right patterning (Levin and Mercola, 1999). Although the importance of gap junctions is well recognized, the functions and mechanisms of action of gap junctions *in vivo* remain largely unknown. The challenge associated with defining gap-junction functions can be attributed to the complexities of connexin assembly and gap-junction networks (Mathews and Levin, 2017; Theis et al., 2005). Distinct types of connexins can potentially form heteromeric and heterotypic gap junctions, which means that different types of connexins could form heterogeneous connexon hexamers. In general, six identical connexins form a homomeric-connexon (Fig. S1B), whereas a mixture of different types of connexins forms a heteromeric-connexon (Fig. S1C). Furthermore, the same types of two homomeric connexons form a homomeric-homotypic (Fig. S1D) or heteromeric-homotypic (Fig. S1E) gap junction, although it is difficult to know whether a heteromeric-homotypic gap junction is actually formed in the manner shown in Fig. S1E. However, different types of two connexons form a homomeric-heterotypic (Fig. S1F) or heteromeric-heterotypic (Fig. S1G) gap junction (Theis et al., 2005). In the case of connexin 41.8 (Cx41.8) and connexin 39.4 (Cx39.4), which are the focus of this study, we have previously shown that these connexins possibly form a homomeric-heterotypic and a heteromeric-homotypic/heterotypic gap junction between *Xenopus* oocytes (Watanabe et al., 2016). In addition, the directional control of gap junctions complicates the gap-junction network. Heterotypic gap junctions occasionally yield a rectifying property, which is caused by the anion/cation selectivity of each connexon (Suchyna et al., 1999), whereas rat Cx40 exhibits polyamine-dependent rectification properties (Musa and Veenstra, 2003). Typically, a homomeric-homotypic gap junction shows bidirectional current flow (Fig. S1D, S1H). In the case of rat Cx40, polyamines, such as spermine and spermidine, were found to bind to the N terminus of connexin and block the outward flow through gap junctions (Lin et al., 2006; Musa et al., 2004). Simply put, polyamine injected into one side of a paired cell generates unidirectional current flow through the gap junction (Fig. S1I), although this has only been detected in *in vitro* experiments.

[1]Graduate School of Frontier Biosciences, Osaka University, 1-3 Yamadaoka, Suita, Osaka 565-0871, Japan. [2]CREST, Japan Science and Technology Agency, 1-3 Yamadaoka, Suita, Osaka 565-0871, Japan.

*Author for correspondence (watanabe-m@fbs.osaka-u.ac.jp)

M.W., 0000-0002-5744-197X

Received 31 May 2019; Accepted 24 October 2019

Development (2019) 146, dev181065. doi:10.1242/dev.181065

The zebrafish possesses yellow and black stripes on its body (Fig. S2A); yellow stripes consist of xanthophores, which have yellow pigments, such as pteridin derivatives (Odenthal et al., 1996), and black stripes consist of melanophores, which have melanin granules in the cells (Milos et al., 1983). In zebrafish, a third type of pigment cell, iridophores, exists, which have a glossy appearance. In the stripe region of the fish body, iridophores spread over and underneath melanophores, whereas in the inter-stripe region, iridophores are located under xanthophores. In fish fins, only a few iridophores exist (Frohnhöfer et al., 2013; Hirata et al., 2003, 2005). All three types of pigment cell are involved in the stripe pattern formation on the trunk of zebrafish (Fadeev et al., 2015, 2016, 2018; Frohnhöfer et al., 2013; Krauss et al., 2013; Lang et al., 2009; Patterson and Parichy, 2013), although iridophores are not involved in the stripe patterning of the fin region (Singh et al., 2015; Watanabe and Kondo, 2015a). The zebrafish stripe is recognized as a highly favorable model for investigating pattern formation in not only experimental studies (Eom et al., 2015; Mahalwar et al., 2014; Singh et al., 2014; Yamanaka and Kondo, 2014) but also in theoretical studies (Nakamasu et al., 2009; Volkening and Sandstede, 2018). A mathematical model, the reaction-diffusion (R-D) model, which was originally presented by Alan Turing, effectively explains pattern formation (Turing, 1952). In this model, two diffusible substances interact with each other to form a pattern. More recently, Meinhardt and Gierer reported that the R-D model for pattern formation requires only a network that includes short-range positive feedback and long-range negative feedback (Meinhardt and Gierer, 1974, 2000), which generates patterns in a cell-autonomous manner. This model effectively reconstructs many biological patterns, e.g. patterns observed in vertebrate skin or on seashells and arrangements of feathers on the bodies of chicks (Kondo and Asai, 1995; Meinhardt, 1995; Prum and Williamson, 2002). Accordingly, among pigment cells in zebrafish, several interactions that generate stripes have been identified (Frohnhöfer et al., 2013; Maderspacher and Nusslein-Volhard, 2003; Mahalwar et al., 2016; Patterson and Parichy, 2013; Takahashi and Kondo, 2008; Yamaguchi et al., 2007; Yamanaka and Kondo, 2014). Repulsive interactions between xanthophores and melanophores, and interactions that mediate activation signaling from xanthophores to melanophores, are crucial for the generation of an equally spaced pattern of stripes by xanthophores and melanophores (Nakamasu et al., 2009; Watanabe and Kondo, 2015b; Yamanaka and Kondo, 2014). Regarding the repulsive interactions, melanophores occur in the yellow stripe region of xanthophores, which are usually eliminated by the repellant movement of melanophores to the melanophore region (Sawada et al., 2018; Takahashi and Kondo, 2008), or are occasionally removed by xanthophores (Nakamasu et al., 2009). This repulsion was effectively reconstructed *in vitro* where the repellant movement of melanophores from xanthophores was observed in culture (Inaba et al., 2012; Yamanaka and Kondo, 2014). At the metamorphosis stage in zebrafish, melanoblasts in the yellow stripe region move to the melanophore region in a macrophage-dependent manner (Eom and Parichy, 2017). The requirement of the activation signal from xanthophore to melanophore was observed *in vivo*. Removal of xanthophore from a region on the trunk of a fish by laser ablation caused the reduction of melanophores surrounding the ablated xanthophore space (Nakamasu et al., 2009). Zebrafish mutants that harbor a temperature-sensitive mutation in *csf1ra* support this feature; the elimination of xanthophores by heat treatment of mutant fish causes the reduction of the number of melanophores on the body of these fish (Parichy et al., 2000; Parichy and Turner, 2003). The involvement of Notch-Delta signaling in the activation signal is expected (Hamada et al., 2014).

We and others have sought to understand the molecular mechanisms underlying this stripe patterning (Eom et al., 2012; Fadeev et al., 2015; Inoue et al., 2014; Iwashita et al., 2006). Recent studies have revealed that gap-junction proteins are crucial molecules for the cell-cell interaction among pigment cells (Irion et al., 2014; Mahalwar et al., 2016; Watanabe et al., 2006, 2016; Watanabe and Kondo, 2012). RT-PCR analysis has previously shown that *cx39.4* and *cx41.8* (*gja5b*) are expressed in both xanthophores and melanophores (Watanabe et al., 2016), and whereas mutations in Cx39.4, a teleost-specific connexin, cause a labyrinth or irregular stripe formation (Fig. S2B) (Irion et al., 2014; Watanabe et al., 2016), a Cx41.8-null mutation generates a spotted pattern (Fig. S2C) (Watanabe et al., 2006) instead of stripes (Fig. S2A). Notably, double knockout of *cx39.4* and *cx41.8* (WKO) causes a loss of the typical skin pattern (Fig. S2D) (Irion et al., 2014; Watanabe et al., 2016). Transplantation experiments clarified that the gap junctions among melanophores and xanthophores are crucial for gap junction-dependent stripe patterning and that iridophores are not involved (Irion et al., 2014; Maderspacher and Nusslein-Volhard, 2003). Furthermore, Cx39.4 and Cx41.8 harbor a predicted polyamine-binding motif in their N-terminal domains that might function in skin pattern formation (Watanabe et al., 2012). Supporting this notion, ectopic overexpression of a spermine/spermidine metabolic enzyme [spermidine/spermine-N(1)-acetyltransferase; encoded by *ssat*] in melanophores perturbed the stripe pattern (Watanabe et al., 2012). Intriguingly, the stripe pattern was also disrupted by the loss of spermidine synthase (encoded by *idefix*) but not spermine synthase, which indicates that spermidine, but not spermine, contributes to stripe-pattern formation in zebrafish (Frohnhöfer et al., 2016).

Here, to elucidate the function of gap junctions in the mechanism underlying stripe pattern formation, we reconstructed the gap-junction network among pigment cells and, ultimately, identified the minimal requirement of connexin expression in pigment cells for stripe formation. Moreover, we performed electrophysiological analyses and detected spermidine-dependent rectification in Cx39.4-containing gap junctions.

RESULTS

The connexin genes *cx39.4* and *cx41.8* are expressed in pigment cells

As noted in the preceding section, Cx39.4 and Cx41.8 are involved in stripe pattern formation, and mutations in these proteins generate labyrinth and spot patterns instead of the typical stripe pattern (Fig. S2A-C). However, whether other connexins are involved in the stripe patterning remains unclear, and expressions of connexins in pigment cells of trunk have not been investigated. To address these issues, we examined connexin expression in melanophores and xanthophores both from the skin and fin. After homogenizing the trunk and fins in adult fish, 100 melanophores and 100 xanthophores were manually collected separately. RNA was extracted from the isolated pigment cells, and cDNA libraries were generated. We then performed RT-PCR and detected that *cx39.4* and *cx41.8* were expressed in melanophores and xanthophores from both the trunk (Fig. 1A) and fin (Fig. 1B) using gene-specific primer sets (Table S1). We did not detect expression of the other connexin genes in melanophores or xanthophores from either the trunk or fin (Fig. S3A,B). Based on these results, we concluded that only *cx39.4* and *cx41.8* are detectably expressed in melanophores and xanthophores.

Development (2019) 146, dev181065. doi:10.1242/dev.181065

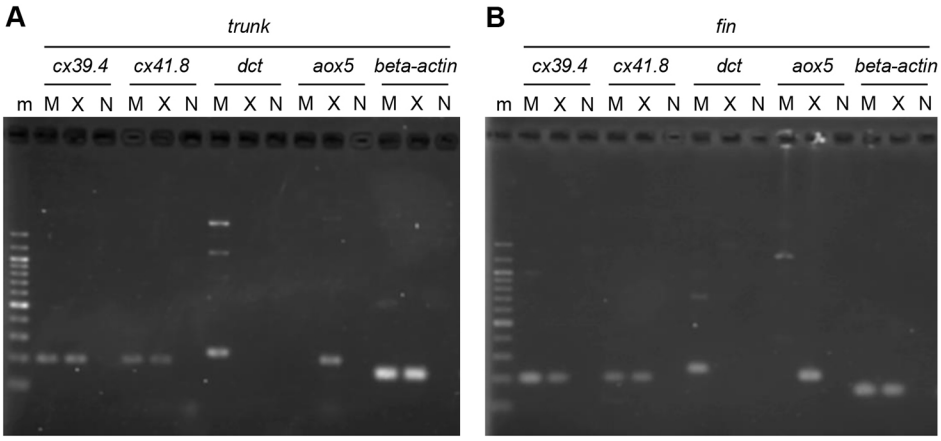

Fig. 1. Connexin expression in pigment cells. (A,B) Expression of *cx39.4* and *cx41.8* in melanophores and xanthophores that were collected from the trunk (A) and fin (B) were analyzed by RT-PCR. m, molecular marker; M, melanophore; X, xanthophore; N, negative control (without cDNA). *dct* and *aox5* were positive controls for melanophore- or xanthophore-specific expression, and β-actin was a positive control for RT-PCR. Two independent experiments were performed and the same results were obtained. RT-PCR results for the other connexins are shown in Fig. S3.

Connexin expression and fish phenotype

To understand connexin/gap-junction functions in pigment cells, we generated transgenic lines expressing Cx39.4 and/or Cx41.8 in melanophores and/or xanthophores. To induce cell type-specific gene expression in melanophores and xanthophores, we used the promoters of *mitfa* (microphthalmia-associated transcription factor a) and *aox5* (aldehyde oxidase 5), respectively (Fig. 2A) (Lister et al., 1999; Parichy et al., 2000). The expression of *mitfa* is occasionally detected in xanthophores (Fig. S2I - S2I″) (Saunders et al., 2019) because xanthophores and melanophores are derived from common progenitor cells, and *mitfa* expression continues during melanoblast differentiation into melanophores (Dooley et al., 2013; Lister et al., 1999; Usui et al., 2018). We used the IRES-H2BRFP fluorescence-reporter cassette to monitor gene expression driven by the *mitfa* or *aox5* promoter [Fig. S2E-H″, S5A-A″ (white arrowheads); RFP (red fluorescent protein) signal marks nuclei in melanophores (Fig. S2E″, F″) and xanthophores (Figs S2G″,H″, S5A″); yellow arrowhead indicates xanthophore autofluorescence (Fig. S2F″)]. By using this system, we collected zebrafish lines that did not show any detectable RFP signal in undesired cells (Figs S2E-H, S5A).

In Fig. 2B-R, we present the phenotypes of wild-type, mutant and transgenic zebrafish lines generated in this study. On the left side of each panel, black and yellow boxes represent melanophores and xanthophores, and green and red small boxes indicate connexons formed by Cx39.4 and Cx41.8, respectively; thus, a pair of two green small boxes indicates homotypic Cx39.4 gap junctions, whereas a pair of green and red boxes indicates heterotypic gap junctions formed by Cx39.4 connexons and Cx41.8 connexons. In this model, the possible formation of heteromeric gap junctions was ignored. In wild-type zebrafish (Fig. 2B), both Cx39.4 and Cx41.8 are expressed in both melanophores and xanthophores, which supports the potential existence of homotypic gap junctions formed by Cx39.4 and Cx41.8, as well as heterotypic gap junctions formed by Cx39.4 and Cx41.8. These heterotypic gap junctions can be of two types: Cx39.4(M)-Cx41.8(X) or Cx39.4(X)-Cx41.8(M) (M or X indicates melanophore or xanthophore, respectively). In Fig. 2C, D, we show the connexin mutants *cx39.4*$^{-/-}$ (*luchs*) and *cx41.8*$^{-/-}$ (*leopard*) (Irion et al., 2014; Watanabe et al., 2006, 2016). In these mutants, Cx39.4 gap junctions or Cx41.8 gap junctions exist among the pigment cells. Fig. 2E shows the double mutant of Cx39.4 and Cx41.8 (WKO or *cx39.4*$^{-/-}$, *cx41.8*$^{-/-}$), which lacks gap junctions among melanophores and xanthophores. To evaluate the effect of the connexins expressed in pigment cells, we quantified and compared the number of melanophores, the stripe width, the spot size and the xanthophore density (Table 1, Fig. 3).

Fig. S4A-I shows representative examples of the variation of fish phenotypes analyzed in Fig. 3. The left column of each panel in Fig. S4 shows maximal/strong phenotypes, and the right column shows minimal/weak phenotypes of melanophores number/width in stripe/spot of each fish line. For example, Fig. S4A shows the variation of stripe width of the wild-type zebrafish, which is reflected as the width of the box chart in Fig. 3D. To simplify the counting of melanophores, melanosomes in melanophores were aggregated with epinephrine, so that the black stripe or spot on the fish trunk appeared bright (Fig. S4A-I). The phenotypes of the mean in width/spot size among each fish line are shown in Fig. 2. In addition, the instability of the fin pattern was particularly noticeable. Fig. S4J-L depict the differences of fin patterns between siblings of wild-type (Fig. S4J) and mutant fish (Fig. S4K,L). Even the wild-type zebrafish occasionally shows a broken stripe pattern (Fig. S4J, right), and two *cx39.4*$^{-/-}$ mutant fish showed different patterns, both in the trunk and fin. This might be because various phenotypes from the same transgenic line were obtained and the recoveries in fin stripe appear incomplete (Fig. 2). Another possibility is that the recovery of the fin pattern was less than that of the trunk, which might be caused by the promoters, making it difficult to compensate for the endogenous promoter activity with *mitfa*- and *aox5*-promoters over a long period of time (>1 month).

We counted the melanophores present within the area demarcated by the red solid line and indicated by the green arrow in Fig. 3A (Fig. 3B,C). Stripe width was measured around the center region of the 1V stripe (Fig. 3A,D) (Hamada et al., 2014). Cluster size of melanophore spots was determined by counting the number of melanophores in each spot (Fig. 3E). Xanthophore densities were measured from four randomly selected areas (~0.5-1.4 mm^2 square) in the X0 yellow stripe, which is demarcated by the red solid line and indicated by the blue arrow (Fig. 3A). The means were calculated in each fish line (Fig. 3F,G). The two regions indicated by blue and green arrows are separated by a purple dotted line, which indicates the myoseptum. Serial numbers were assigned to the transgenic fish as Tg-1–Tg-14 (Fig. 2, Figs S2, S5).

Single expression of Cx39.4 or Cx41.8 in double-knockout mutant

In Fig. 2F-I, Tg-1–Tg-4 represent the phenotypes of transgenic zebrafish in WKO background in which Cx39.4 or Cx41.8 expression was induced using pigment cell-specific promoters (as indicated): Cx39.4 was expressed in either melanophores (Fig. 2F, Fig. S4B) or xanthophores (Fig. 2H, Fig. S4C), and Cx41.8 was expressed in either melanophores (Fig. 2G) or xanthophores

Development (2019) 146, dev181065. doi:10.1242/dev.181065

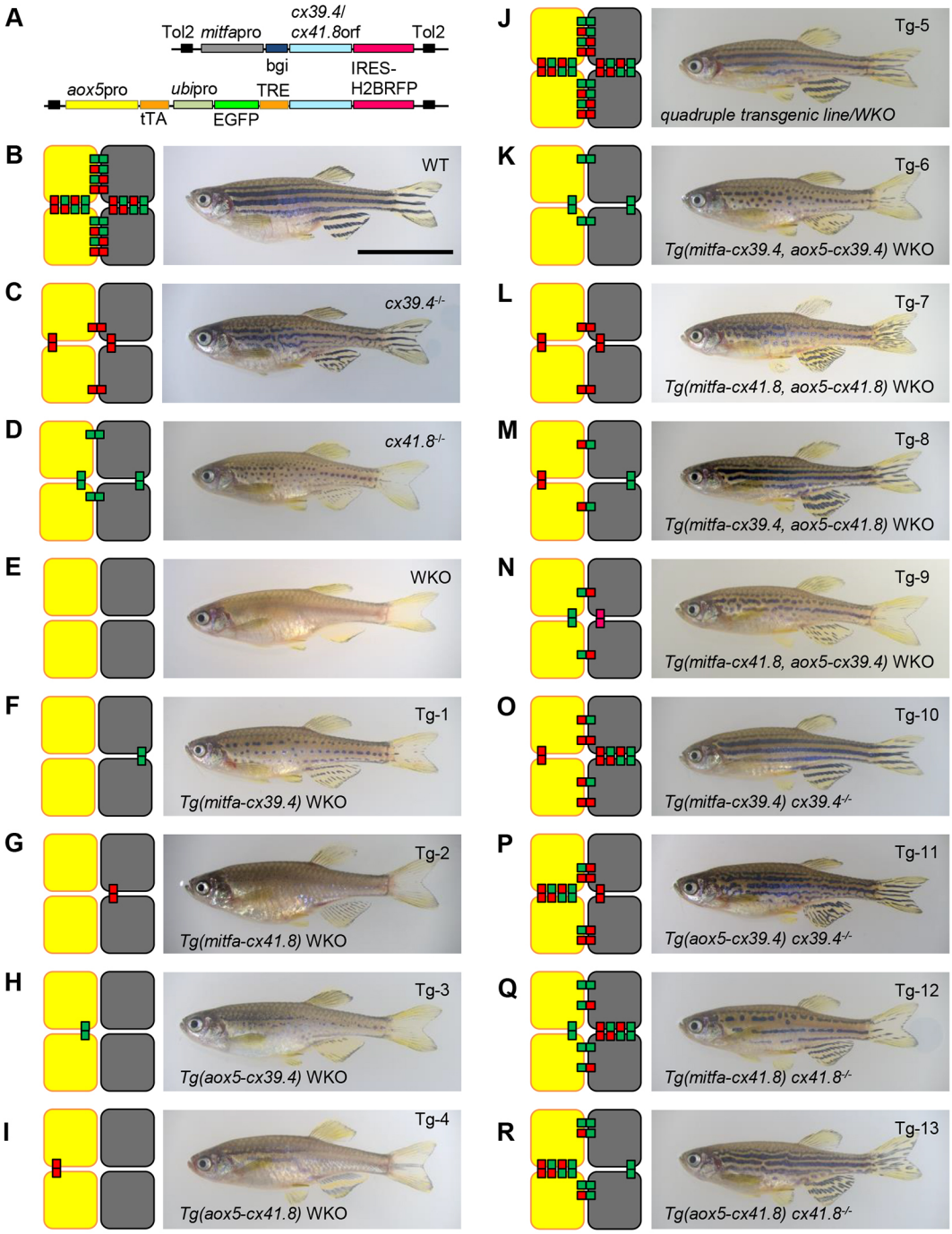

Fig. 2. Mutant and transgenic fish lines, and reconstructed gap junction networks. (A) Plasmid construct designs: *mitfa* promoter (A; upper line) and *aox5* promoter (A; lower line) were used for pigment-cell-specific gene expression. tTA/TRE was used to enhance *aox5* promoter activity, and an *ubi*pro (*ubiquitinb* promoter)-EGFP cassette was used to simplify the genotyping of fish embryos. The fragments were cloned into a pTol2 plasmid, and each plasmid was used to generate transgenic zebrafish. (B-R) The reconstructed gap junction network (left) and a representative photograph of a fish from the corresponding line (right). Wild-type (B; WT), *cx39.4*$^{-/-}$ (C; *luchs*), *cx41.8*$^{-/-}$ (D; *leopard*) and double-knockout mutant (E; WKO), and transgenic zebrafish lines in WKO background (F-N; Tg-1 to Tg-9), *cx39.4*$^{-/-}$ background (O,P; Tg-10 and Tg-11) and *cx41.8*$^{-/-}$ background (Q,R; Tg-12 and Tg-13). *mitfa* promoter (F,G,O,Q) and *aox5* promoter (H,I,P,R) were used to induce *cx39.4* or *cx41.8* in pigment cells. Double (K-N) and quadruple (J) transgenic lines were generated by means of crossing among mutant and transgenic lines. Gene expression in unexpected cells was monitored using IRES-H2BRFP fluorescent protein (Fig. S2). Scale bar: 10 mm.

(Fig. 2I, Fig. S4D). Cx39.4 expression in melanophores (Tg-1) restored the WKO phenotype to the skin pattern present in *cx41.8*$^{-/-}$ (Fig. 2D-F). Not only was the melanophore density on the fish trunk restored but so was the size of each spot, as in *cx41.8*$^{-/-}$ (Table 1, Fig. 3B,E). This result indicates that Cx39.4 functions not between melanophores and xanthophores but between melanophores; however, the possibility remains that Cx39.4 also forms gap junctions with unidentified connexons on other cells or functions solely as a hemichannel. By contrast, single Cx41.8 expression in melanophores (Tg-2) was insufficient for pattern formation

Development (2019) 146, dev181065. doi:10.1242/dev.181065

Table 1. Melanophore densities on fish trunk

Genotype	Melanophores/mm^2	s.d.	*n*	Tg number in Fig. 2	Panel in Fig. 2
Wild type	67.78	6.65	10		B
cx39.4$^{-/-}$	36.51	4.28	10		C
Tg(mitfa-cx39.4)cx39.4$^{-/-}$	52.30	9.16	7	Tg-10	O
Tg(aox5-cx39.4)cx39.4$^{-/-}$	43.29	4.68	4	Tg-11	P
cx41.8$^{-/-}$	25.94	5.23	10		D
Tg(mitfa-cx41.8)cx41.8$^{-/-}$	38.34	4.94	10	Tg-12	Q
Tg(aox5-cx41.8)cx41.8$^{-/-}$	69.58	8.95	10	Tg-13	R
WKO	2.56	2.15	10		E
*Tg(mitfa-cx39.4)*WKO	24.25	6.48	18	Tg-1	F
*Tg(mitfa-cx41.8)*WKO	8.61	3.00	10	Tg-2	G
*Tg(aox5-cx39.4)*WKO	21.56	5.30	10	Tg-3	H
*Tg(aox5-cx41.8)*WKO	35.18	6.72	18	Tg-4	I
*Tg(mitfa-cx39.4, aox5-cx39.4)*WKO	18.54	2.80	10	Tg-6	K
*Tg(mitfa-cx41.8, aox5-cx41.8)*WKO	23.77	5.28	16	Tg-7	L
*Tg(mitfa-cx39.4, aox5-cx41.8)*WKO	55.46	7.68	11	Tg-8	M
*Tg(mitfa-cx41.8, aox5-cx39.4)*WKO	23.86	2.95	4	Tg-9	N
Tg(mitfa-cx39.4, mitfa-cx41.8, aox5-cx39.4, aox5-cx41.8)WKO	54.26	9.09	5	Tg-5	J

The number of melanophores per body surface area is shown. Adult stage fish (standard length: 26.13±1.63 mm) were used for the cell counting.

(Fig. 2G). In this fish, we observed no change in phenotype from that of WKO. In the case of single expression of Cx39.4 or Cx41.8 in xanthophores (Tg-3, Tg-4), the mutant phenotype was not restored, although melanophore numbers (Fig. 2H,I, Fig. S4C,D) and xanthophore densities (Fig. 3G) were increased (Table 1). Given this, we hypothesized that gap junctions in xanthophores might function as adhesion molecules in order to make the xanthophore area compact, which would allow melanoblasts in the free space to readily differentiate without interference from xanthophores. To confirm this, we expressed Cx43 in xanthophores (Fig. S5A-A″), which revealed that xanthophore density was increased, although the recovery of xanthophore density was small (Fig. S5B). Intriguingly, Cx43 expression did not cause recovery of the number of melanophores (Fig. S5A).

Reconstruction of gap junction network required for stripe pattern formation

By means of mating among the transgenic lines Tg-1–Tg-4 (Fig. 2F-I) or by mating them with the mutant lines *cx39.4*$^{-/-}$ or *cx41.8*$^{-/-}$, we generated double and quadruple transgenic lines in a WKO background (Tg-5–Tg-9; Fig. 2J-N) and single-knockout background (Tg-10–Tg-13; Fig. 2O-R). As expected, quadruple-transgenic zebrafish showed the stripe pattern (Tg-5; Fig. 2J). This result supports the view that Cx39.4 and Cx41.8 expression in melanophores and xanthophores was sufficient, and that the expression of these connexins in other cells was not necessary for stripe formation in the WKO-background fish. Intriguingly, in Tg-5, the black stripe was thinner than that in wild type, but the underlying reason remains unclear (Figs 2J and 3D).

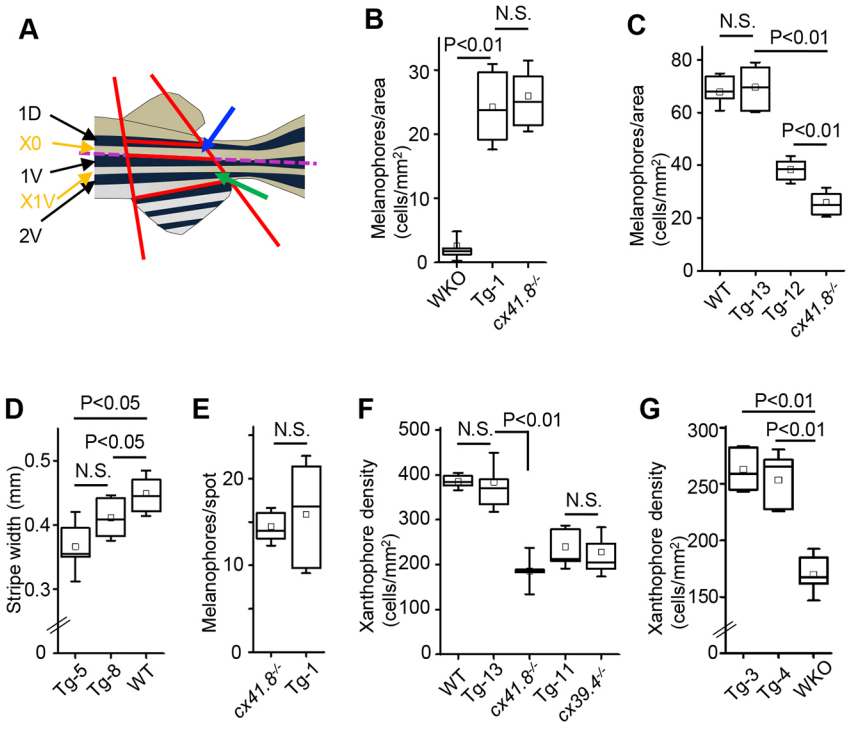

Fig. 3. Effect of connexin(s) on pigment cell behavior and distribution. (A) Melanophores in the trunk area that are located between the solid red lines and indicated by the green arrow were counted. The purple dotted line indicates the myoseptum. Xanthophore densities were measured from four randomly selected areas (~0.5-1.4 mm^2) in the X0 stripe, which is demarcated by two solid red lines and indicated by a blue arrow. (B,C) Melanophore numbers compared among WKO, Tg-1 and *cx41.8*$^{-/-}$ (B), and WT, Tg-13, Tg-12 and *cx41.8*$^{-/-}$ (C). (D) Stripe width compared in Tg-5 (0.466±0.048 mm, *n*=5), Tg-8 (0.511±0.034 mm, *n*=11) and WT (0.549±0.034 mm, *n*=11). (E) The number of melanophores per spot compared in *cx41.8*$^{-/-}$ (14.58±2.06 cells/spot, *n*=5) and Tg-1 (15.86±6.58 cells/spot, *n*=5). Melanophores were counted in 20 spots per fish and the means calculated. (F) Xanthophore densities in single-mutant backgrounds: WT, 385.24±17.15 cells/mm^2 (*n*=5); Tg-13, 383.60±28.63 cells/mm^2 (*n*=5); *cx41.8*$^{-/-}$, 185.81±49.08 cells/mm^2 (*n*=5); Tg-11, 242.77±44.37 cells/mm^2 (*n*=5); *cx39.4*$^{-/-}$, 228.24±17.98 cells/mm^2 (*n*=5). (G) Xanthophore densities compared in WKO (169.71±20.35 cells/mm^2, *n*=5), Tg-3 (253.39±17.98 cells/mm^2, *n*=5) and Tg-4 (263.17±17.98 cells/mm^2, *n*=5). *P*-values (Student's *t*-tests) are shown within graphs; N.S., not significant (*P*>0.05). Intermediate lines in each box are median values and small squares are means. The box limits indicate the first and third quartiles; lines and whiskers indicate the mean±s.d.

Development (2019) 146, dev181065. doi:10.1242/dev.181065

Next, we examined the effects of connexin pairs expressed between melanophores and xanthophores. When Cx39.4 was expressed in both melanophores and xanthophores in the WKO background (Tg-6), the spot pattern was generated as in *cx41.8*$^{-/-}$ (Fig. 2D,K). This agrees with the result obtained with Tg-1. Conversely, when Cx41.8 was expressed in both melanophores and xanthophores (Tg-7), the WKO phenotype was effectively restored to the *cx39.4*$^{-/-}$ phenotype (Fig. 2L), which indicates that *mitfa* and *aox5* promoters compensated for the *cx41.8* promoter in melanophores and xanthophores (Watanabe and Kondo, 2012). Tg-8, in which Cx39.4 was expressed in melanophores and Cx41.8 was expressed in xanthophores, showed the stripe pattern (Fig. 2M). This key finding forms the basis for the conclusion of this study that, for stripe formation, the minimal requirement of connexin expression in pigment cells is Cx39.4 in melanophores and Cx41.8 in xanthophores. However, the black stripe in Tg-8 was thinner than that in wild type (Fig. 3D), and the stripe in the fin was incomplete. The Tg-9 phenotype appeared intermediate between the Tg-7 and Tg-8 phenotypes, featuring partially broken and narrow stripes (Fig. 2N), although this phenotype was not particularly informative because, as noted above, Cx41.8 expression in xanthophores is necessary for generating stripes. The Tg-10 phenotype strongly supported the conclusion here regarding the requirement of Cx41.8(X)-Cx39.4(M) (Fig. 2O), and in Tg-10, the stripe pattern was clearer than that in Tg-8, which suggests that Cx41.8 expressed in melanophores performs a supportive function in stripe formation. Tg-11 fish showed wavy and partially broken stripes as in the *cx39.4*$^{-/-}$ mutant (Fig. 2P), and the xanthophore density in Tg-11 was almost the same as that in *cx39.4*$^{-/-}$ (Fig. 3F). This agrees with the result indicating that Cx39.4 expression in xanthophores is not required. The phenotype of Tg-12 was the same as that reported previously (Figs 2Q and 3C) (Watanabe and Kondo, 2012), although individual fish showing broken stripes to large spot patterns were also obtained. Tg-13 satisfied the connexin expression required for stripe formation, but the stripes were partially broken and narrower than in wild type (Fig. 2R). Cx41.8 might be necessary for generating narrow/normal interstripes. When Cx39.4 was co-expressed with Cx41.8 in xanthophores, the stripe pattern was unstable, and the spots or stripes were smaller or narrower than those in transgenic fish expressing only Cx41.8 in xanthophores (Tg-10 versus Tg-5, Tg-8 versus Tg-13).

Visualization of Cx39.4 *in vivo* and *in vitro*

In previous studies, we predicted that gap junctions mediate signal transfer from xanthophores to melanophores, and that this represents a cue provided by the gap junction network for pattern formation (Watanabe et al., 2012). Here, we sought to perform electrophysiological analysis of Cx39.4 gap junctions by using the patch clamp technique to determine whether Cx39.4 expressed in melanophores possesses a rectification property and exhibits the ability to control the direction of signal transfer through gap junctions. First, we designed a plasmid construct that expresses EGFP-tagged Cx39.4 and thus allows gap junction plaque visualization *in vitro* and *in vivo*. We cloned the gene encoding the fusion protein composed of Cx39.4 (full-length ORF) and EGFP in pIRES2-DsRed vector and transfected the plasmid into HeLa and Neuro2A (N2a) cells. In parallel, we introduced the gene encoding EGFP-tagged Cx39.4 into the *cx39.4*$^{-/-}$ mutant by using the same method described in Fig. 2A. We found that EGFP-tagged Cx39.4 did not function *in vivo* or *in vitro*: EGFP-tagged Cx39.4 neither formed gap junction plaques between cultured cells nor restored the *cx39.4*$^{-/-}$ mutant phenotype of zebrafish (data not shown). We struggled to find the construct of functional EGFP-tagged Cx39.4. In humans, plaque formation of GFP-tagged C-terminal truncated Cx37 has been reported (Kumari et al., 2000). Referring to this, we added an EGFP tag to the 256th position on Cx39.4, generating Cx39.4del$_{256\text{-}341}$EGFP. In this case, we found that fewer than 10% of N2a cell pairs formed a gap junction plaque between N2a cells (data not shown). Next, expecting the improvement of plaque formation rate, we added the C-terminal fragment of Cx39.4 at the C terminus of the EGFP sequence in Cx39.4del$_{256\text{-}341}$EGFP because putative ZO-1 binding residues are included in the C-terminal region of Cx39.4, and the importance of the ZO-1 binding domain for Cx39.4 function has been predicted (Fadeev et al., 2015). Consequently, we obtained a construct encoding Cx39.4exc$_{256\text{-}321}$EGFP, in which a 66-residue stretch, from amino acids 256 to 321, at the C-terminal domain of Cx39.4 was exchanged with the EGFP fragment (Cx39.4exc$_{256\text{-}321}$EGFP) (Fig. 4A). We confirmed that Cx39.4exc$_{256\text{-}321}$EGFP was functional *in vivo*: Cx39.4exc$_{256\text{-}321}$EGFP expression, which was driven by a *mitfa* promoter, restored the *cx39.4*$^{-/-}$ mutant phenotype (Fig. 4B). Furthermore, the EGFP signal was observed in cells and localized at cell membranes, and gap junction plaques were detected between melanophores (arrowhead in Fig. 4C; compared with negative control in Fig. 4D). This gene fragment was also cloned into the pIRES2-DsRed vector for transfection of cultured cells, and our results revealed successful formation of gap junction plaques between N2a cells (Fig. 4E,E′); however, gap junction plaques could not be detected between transfected HeLa cells.

The spermidine-dependent rectification property of Cx39.4 gap junctions

Zebrafish connexins rarely assemble on the mammalian cell membrane, which precludes precise analysis of their gap junction properties; therefore, the oocyte-clamp technique is typically used for studying zebrafish gap junctions (Hoptak-Solga et al., 2007; Klaassen et al., 2016; Misu et al., 2016; Watanabe et al., 2016). The oocyte-clamp technique offers the advantage that a large current value is obtained when compared with that in patch-clamp experiments; however, analyzing polyamine sensitivity of gap junctions using this method is challenging. The large volume of an oocyte (estimated as 1 µl compared with the 1 pl volume of a HeLa cell) (Ferrell and Machleder, 1998; Fujioka et al., 2006) prevents the analysis of polyamine sensitivity to gap junctions. Thus, no previous study has successfully examined the polyamine sensitivity of zebrafish gap junctions. Here, we were able to reconstruct gap junction plaques and visualize Cx39.4 gap junctions between N2a cells, and we therefore used this system to perform patch-clamp experiments. At 24-72 h post-transfection, we selected, for analyses, pairs of N2a cells exhibiting the EGFP signal as an indicator of gap junction plaques. We clamped both cells initially at −40 mV and applied a series of transjunctional voltages (Vi, −140 to +60 mV in 20 mV increments) to one of the cells and recorded the transjunctional current (Ij) in the other cell (Fig. 4F,G; upper set of lines in Fig. 4G). Fig. 4G presents examples for each experimental condition. As a negative control, we used cell pairs that were not transfected with the plasmid, and we detected no currents here (Fig. 4G, second set of lines). In Fig. 4G, the third line represents transjunctional current traces of Cx39.4 gap junctions. As previously shown in voltage-clamp experiments performed using *Xenopus* oocytes, slow deactivation of gap junctions was observed (Watanabe et al., 2016).

Development (2019) 146, dev181065. doi:10.1242/dev.181065

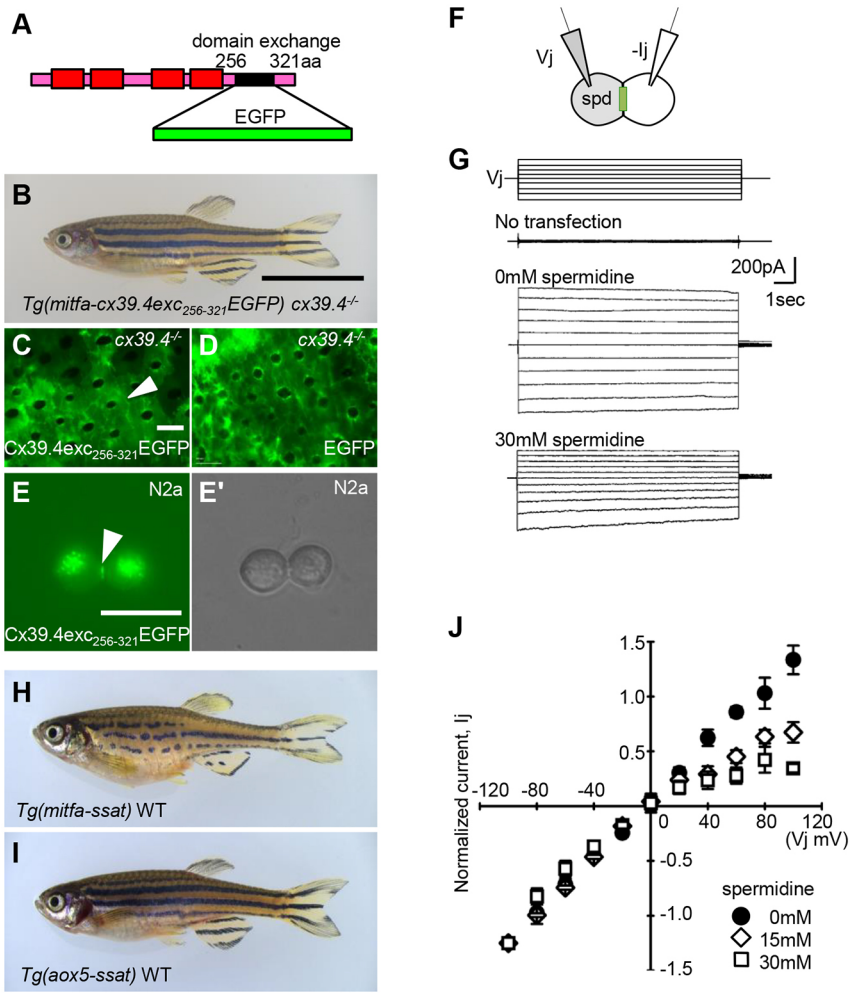

Fig. 4. Visualization and characterization of Cx39.4. (A) Schematic of EGFP-tagged Cx39.4. Cx39.4 C-terminal sequence from amino acids 256 to 321 was exchanged with the EGFP fragment. (B) Cx39.4$_{exc256-321}$EGFP was expressed in melanophores of *cx39.4*$^{-/-}$ mutant zebrafish. The mutant phenotype was restored to the stripe pattern after expression. (C) Fluorescence image of transgenic fish skin at F0 generation in *cx39.4*$^{-/-}$ mutant zebrafish; white arrowhead indicates gap junction plaque between melanophores. (D) Control: EGFP was expressed in melanophores of *cx39.4*$^{-/-}$ mutant zebrafish; no EGFP signal was detected between melanophores. (E,E′) Transfected N2a cells: fluorescence (E) and bright-field (E′) microscopy images; white arrowhead indicates a gap junction plaque. (F) Schematic of patch-clamp experiment with spermidine (spd) treatment. (G) Both N2a cells were clamped at −40 mV and a series of transjunctional voltages (Vi, −140 to +60 mV, 20 mV increment) was applied to one of the cells (first trace), and transjunctional current (Ij) was recorded in the other cell with or without spermidine treatment (third and fourth traces). As a negative control, untransfected cells were used (second trace). (H,I) The polyamine metabolic enzyme Ssat (Sat1b) was ectopically expressed in melanophores (H) and xanthophores (I). (J) I-V plot showing the relationship between normalized steady-state junctional currents and transjunctional voltages for 0 mM, 15 mM and 30 mM spermidine treatment. Each data point represents the mean±s.d. for each Vj value (n=5). Vj=Vpre–Vpost (−40 mV). Scale bars: 10 mm in B,H,I; 100 µm in C,D; 20 µm in E,E′.

Next, we examined the polyamine-dependent rectification property of Cx39.4 gap junctions. The contribution of polyamines to zebrafish skin pattern formation has been investigated. As mentioned in the introduction, ectopic overexpression of *ssat* in melanophores perturbs the stripe pattern (Fig. 4H) (Watanabe et al., 2012), and *ssat* expression in xanthophores does not affect skin patterning (Fig. 4I). In mammals, two ssat genes, *ssat1* and *ssat2*, exist in the genome. SSAT1 is related to polyamine metabolism, whereas SSAT2 is not (Coleman et al., 2004; Vogel et al., 2006). In zebrafish, three *ssat1* homologs, *sat1a.1*, *sat1a.2* and *sat1b*, exist (Lien et al., 2013). We performed RT-PCR to investigate gene expression of three *ssat1* genes in pigment cells and found that only *sat1a.2* is expressed in melanophores and xanthophores (Fig. S6). This result indicates that Sat1a.2 may function in homeostasis of melanophores and xanthophores, and the disturbance of its function in melanophores caused an irregular stripe patterning. Moreover, loss of spermidine synthase (*idefix*), but not of spermine synthase, was shown to disrupt the stripes, which indicated that spermidine but not spermine is involved in stripe pattern formation in zebrafish (Frohnhöfer et al., 2016). Thus, we analyzed the spermidine sensitivity of Cx39.4 by adding 15 or 30 mM spermidine into the pipette solution and recorded transjunctional currents by using the same procedure as described in the preceding paragraph. Notably, our results demonstrated asymmetric gap junction gating (Fig. 4G, bottom two sets of lines; Fig. 4J, normalized I-V curve). Thus, we conclude that Cx39.4 exhibits dose-dependent spermidine sensitivity.

DISCUSSION

To elucidate the function of gap junctions in pattern formation in zebrafish skin, we reconstructed the gap junction network among pigment cells. By controlling the expression of the connexins Cx39.4 and Cx41.8 specifically in melanophores and xanthophores (Fig. 2), we determined that the minimal requirement of connexin expression for stripe pattern formation is Cx39.4 in melanophores and Cx41.8 in xanthophores. Furthermore, we successfully generated an EGFP-tagged Cx39.4 construct that formed gap junction plaques *in vitro* and restored the mutant phenotype *in vivo*. Last, by using this EGFP-tagged Cx39.4 construct and the patch-clamp technique, we showed that Cx39.4 gap junctions exhibit a spermidine-dependent rectification property. However, spermidine sensitivity of Cx41.8 gap junctions has not been examined because Cx41.8 does not form gap junction plaques between cultured cells. Instead, previously we used rat Cx40, a mammalian orthologue of Cx41.8, to examine the necessity of the polyamine-binding motif at the N terminus of connexin (Watanabe et al., 2012). Rat Cx40 is reported to be blocked by 5-15 mM spermidine (Musa and Veenstra, 2003) and an amino acid substitution at the polyamine-binding motif inhibits the rectification property of the rat Cx40 gap junction (Lin et al., 2006; Musa et al., 2004). We showed the polyamine-binding motif on rat Cx40 is required for the stripe pattern formation of zebrafish in the cross-species transgenic experiments (Watanabe et al., 2012), which supports that connexins expressed in melanophores require polyamine-binding

Development (2019) 146, dev181065. doi:10.1242/dev.181065

properties for the stripe pattern formation. According to our previous mathematical and experimental models for stripe pattern formation, the signal that is required for melanophore survival is transferred from xanthophores to melanophores. Here, we show the possibility that this signal could be transferred from xanthophores to melanophores through a heterotypic gap junction, which was made by a docking Cx41.8-connexon in xanthophores with Cx39.4-connexon in melanophore and has spermidine-dependent rectification properties. The phenotypes from the transgenic experiment in which Cx41.8 was expressed in melanophores may have a function in stabilizing the stripe.

In Fig. 5, we present a model for the gap junction network among pigment cells. In this model, Kir7.1 is also described because it is sensitive to spermidine and crucial for skin pattern formation (Inaba et al., 2012; Iwashita et al., 2006). We found here that 30 mM spermidine blocked outward flow through the Cx39.4 gap junctions. However, the concentration at which spermidine blocks zebrafish Kir7.1 has not been determined. In terms of the effect of spermidine on Kir-family potassium channels, the effective spermidine concentration measured for Kir2.1 was 0.1-50 µM, which blocked the outward flow of potassium ions through the channel (Liu et al., 2012). Previous examination of spermidine concentrations and distribution in cells revealed that the spermidine concentration in the atrium and ventricle in total was ∼100 µM, and that the free spermidine concentration in cells was ∼10 µM (Miyamoto et al., 1993; Watanabe et al., 1991). The spermidine concentration in melanophores is currently unknown, as is the number of spermidine molecules that colocalize with gap junctions at the cell membrane and block gap junction function; however, Cx39.4 and Cx41.8 gap junctions might be blocked partially and over time, to different extents, because the spermidine sensitivities of these two types of gap junctions were found to be lower than that of Kir potassium channels and the spermidine concentration is expected to be ∼100 µM in melanophores. This insufficient blockage of gap junctions might enable signal molecules to spread among melanophores through Cx39.4 gap junctions. In the model presented in Fig. 5, melanophores are shown to extend long projections. Previously, we observed that long filopodia from melanophores extended to xanthophores, and we hypothesized that melanophores use these filopodia to make direct contact with xanthophores at the adult stage in zebrafish (Hamada et al., 2014). Because gap junctions are formed between cells and mediate direct cell-cell interaction, Cx41.8(X)-Cx39.4(M) gap junctions could exist at the tips of melanophores (Fig. 5).

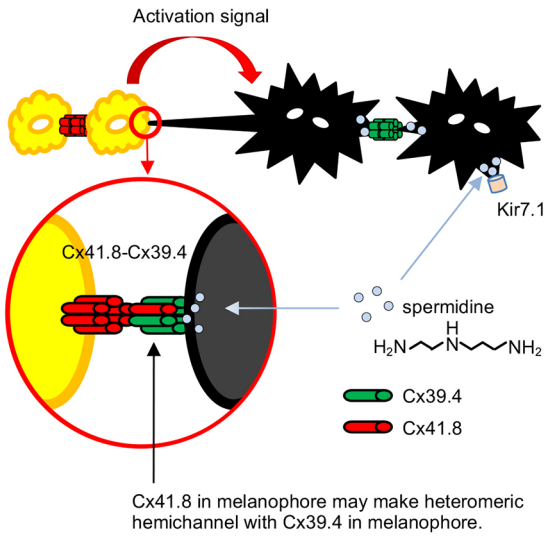

Fig. 5. Hypothesized minimal gap junction network among pigment cells. The minimal connexin expression required for stripe pattern formation is Cx39.4 in melanophores (M) and Cx41.8 in xanthophores (X). Gap junctions formed by Cx41.8(X) and Cx39.4(M) transfer activation signals from xanthophores to melanophores, as predicted by experimental and theoretical studies (Irion et al., 2014; Mahalwar et al., 2016; Watanabe and Kondo, 2012; Watanabe et al., 2016). Cx41.8 expressed in melanophores might assist with Cx39.4 function (see main text). Spermidine in melanophores inhibits outward flow from melanophores through gap junctions and also inhibits Kir7.1, a potassium channel (Watanabe et al., 2012).

In terms of function, Cx39.4 and Cx41.8 were found to play divergent roles in pattern formation in the two types of pigment cells. When Cx39.4 or Cx41.8 was expressed only in melanophores, markedly distinct phenotypes appeared (Fig. 2F,G), although why Tg-1 and Tg-2 fish showed such phenotypes is unclear. Previous comparison of the electrophysiological properties of Cx39.4 and Cx41.8 gap junctions (Watanabe et al., 2016) revealed that Cx41.8 gap junctions exhibit higher sensitivity to transjunctional voltage and more rapid time-dependent inactivation relative to Cx39.4 gap junctions. Moreover, as noted above, the efficiency with which spermidine blocks these two types of gap junctions might differ, and this property would result in divergent effects being produced on the cell-cell communication between melanophores, even in the presence of spermidine. Conversely, when Cx39.4 or Cx41.8 was expressed only in xanthophores, the number of melanophores was increased, although the increase rate differed (Table 1, Fig. 2H,I). Regarding this matter, we investigated the possibility that gap junctions in xanthophores might function as adhesion molecules. Ectopic expression of Cx43 in xanthophore partially recovered the density of xanthophore; however, the number of melanophores was not restored (Fig. S5). Further investigation is required to define how Cx41.8 in xanthophores contributes to the development of melanophores.

In this study, several conditions that might be important for gap junction formation were ignored to simplify the study model. For example, the possibility exists that Cx41.8 or Cx39.4 forms heterotypic gap junctions with other connexin-connexon channels in other cells. Tjp1a mutant zebrafish (*schachbrett*), in which a mutation is present in the protein ZO-1a, showed a spotted pattern similar to that in the *cx41.8*$^{-/-}$ mutant (Fadeev et al., 2015). The PDZ domain in ZO-1 bound to the C terminus of Cx41.8 and Cx39.4, which raised the possibility that Cx41.8 or another connexin in iridophores contributes to the pattern formation (Fadeev et al., 2015). However, our results here indirectly contradict the notion that Cx39.4 or Cx41.8 expression in iridophores is not required for pattern formation (Irion et al., 2014; Maderspacher and Nusslein-Volhard, 2003; Mahalwar et al., 2016). Although large-scale mutant screening of zebrafish has not revealed the involvement of other connexins in pattern formation, further investigation might yield clues to resolving the issue of whether a third connexin in surrounding cells is involved in skin pattern formation.

MATERIALS AND METHODS

Zebrafish husbandry

All experiments were approved by the Animal Experiments Committee and Gene Modification Experiments Safety Committee of Osaka University (permit numbers 04294 and FBS-14-002-1). Zebrafish (*Danio rerio*) were maintained under standard conditions at 28.5°C and a 14/10 h light/dark cycle.

RT-PCR

Pigment cells were collected as previously described (Yamanaka and Kondo, 2014). Briefly, three tail fins were cut off from anesthetized adult zebrafish and washed with phosphate-buffered saline (PBS); the fin clips

Development (2019) 146, dev181065. doi:10.1242/dev.181065

were then treated with a trypsin solution [2.5 mg/ml trypsin (TRL; Worthington), 1.2 mg/ml bovine serum albumin (BSA) (Sigma) and 1 mM EDTA in PBS] for 1 h at 28°C. After washing five times with PBS, the fin clips were treated with collagenase solution [1 mg/ml collagenase I (Worthington), 0.1 mg/ml DNase I (Worthington), 0.1 mg/ml soybean trypsin inhibitor (Worthington) and 1.2 mg/ml BSA in PBS] for 1 h at 28°C. To isolate the trunk pigment cells, fish skin was peeled off from anesthetized zebrafish, using scissors and forceps, and washed with PBS. The collected skin was dissected into ∼3 mm squares with a knife and then treated with the trypsin solution for 20 min at 28°C. After washing five times with PBS, the dissected skin fragments were treated with the collagenase solution for 20 min at 28°C. Next, melanophores and xanthophores from the fin or trunk, respectively, were manually collected individually from the collagenase-treatment solution by using glass capillaries. In each experiment, 100 melanophores or 100 xanthophores were collected from both the trunk and fin. Other organs, including the brain, eye, intestine, ovary and testis, were also collected using forceps. mRNAs were purified from the cells and organs by using an RNeasy purification kit (Qiagen) and used for cDNA library synthesis. RT-PCR was performed using connexin-specific or ssat-specific primers (Table S1). *actb1* (encoding β-actin) was the positive control for RT-PCR, and *aox5* was the positive control of the xanthophore-specific marker genes. *dct* was used as a melanophore-specific marker gene instead of *mitfa* because *mitfa* is occasionally expressed both in melanophores and xanthophores (Dooley et al., 2013; Lister et al., 1999; Usui et al., 2018). cDNAs synthesized from RNA isolated from brain, eye, testis, ovary and skin tissues were used for positive controls to check gene-specific primer sets.

Transgenic fish

Transgenic fish were generated as reported previously. Briefly, the Tol2 transposon-based transgenesis system was used, and 1.5 kb of *mitfa* promoter and 1.7 kb of *aox5* promoter were used to induce connexins (Lister et al., 1999; Parichy et al., 2000). Connexin-coding fragments were PCR amplified (Watanabe et al., 2016) and cloned into the pTol2 plasmid (Kawakami et al., 1998, 2000).

The primer set used to generate *cx43* clones from zebrafish genomic DNA was: cx43_SalI_F, AAAGTCGACGCCACCATGGGTGACTGGAGTGCGTT; and cx43_NotI_R, AAAGCGGCCGCTAGACGTCCAGGTCAG. Amplified fragments were digested with SalI and NotI, and then ligated into pTol2-*aox5* promoter plasmid. To generate pTol2-cx39.4exc$_{256\text{-}321}$EGFP plasmid, three fragments, zfcx39.4N (N-terminal domain), EGFP cassette and zfcx39.4CT (C-terminal domain) sequences were amplified, respectively, using three primer sets: zfcx39.4N (zfcx394EcoF, AAATTTGAATTCGCCACCATGTCCAGAGCTGACTGGGG; and zfcx39.4N255EGFPR01, TCCTCGCCCTTGCTCACCATCACCTCTGCCTGATATTTCTTCTCT); EGFP (39.4N255EGFPF01, AGAAATATCAGGCAGAGGTGATGGTGAGCAAGGGCGAGGAGCTGT; and 394_GFPN321R02, TTTAGGAAGATTGTTTTTGTTCTTGTACAGCTCGTCCATGC); and zfcx39.4CT (39.4EGFPN321F02, GCATGGACGAGCTGTACAAGAACAAAAACAATCTTCCTAAA; and zfcx394NotR01, AAATTTGCGGCCGCTCAAACATAATGTCTCGGTT). The amplified fragments were mixed and re-amplified using the primer set zfcx394EcoF and zfcx394NotR01 to generate a full-length cx39.4exc$_{256\text{-}321}$EGFP fragment. The 1.6 kb fragment obtained was then digested with EcoRI and NotI, and cloned with a pTol2 plasmid vector.

Total RNA was extracted from fish brain by using the RNeasy kit, and a brain cDNA library was generated through reverse transcription performed using Super Script III (Invitrogen). The following primers were used to generate a *sat1b* clone from the brain cDNA library: sat1b_SalI_F, AAAGTCGACGCCACCATGGCCAATTTTAATTTGCG; and sat1b_NotI_R, AAAGCGGCCGCTCACTCTTCAGCAGACATTTTC. Amplified fragments were digested with SalI and NotI, and then individually ligated into a pTol2 plasmid. Transgenic zebrafish lines were generated as described previously (Kawakami et al., 1998, 2000).

Pigment-cell counting

To count melanophores, epinephrine-treated zebrafish were photographed under an MZ16FA stereoscopic microscope (Leica). Epinephrine (10 mM) was used to aggregate melanosomes in melanophores, which facilitates counting. Melanophore numbers and xanthophore densities were calculated using the measurement and particle analyzer features of ImageJ software. Magnified and high-resolution bright-field images of xanthophores were acquired using a BZ-X710 inverted microscope (Keyence).

Electrophysiology

The mouse neuroblastoma cell line Neuro2A (N2a, JCRB Cell Bank) was used for electrophysiological experiments. N2a cells were maintained in Dulbecco's modified essential medium supplemented with nonessential amino acids, antibiotics and 10% fetal bovine serum (Hyclone). The cx39.4exc$_{256\text{-}321}$EGFP fragment (in which a part of Cx39.4 C-terminal domain, from the 256th to 321st amino acid, was exchanged with an EGFP fragment) was subcloned into a pIRES2-DsRed vector (Clontech) using the following primer set: cx39.4_EcoRI_F, CTTCGAATTCGCCACCATGTCCAGAGCTGACTGGG; cx39.4_BamHI_R, TTTGGATCCTCAAACATAATGTCTCGGT. N2a cells were transfected with pIRES2-cx39.4exc$_{256\text{-}321}$EGFP plasmid by using the FuGENE transfection reagent (Promega) according to the manufacturer's instructions, and Cx39.4exc$_{256\text{-}321}$EGFP expression in N2a cells was detected using fluorescence microscopy at 24 h post-transfection. The N2a cells were washed three times with PBS and then placed on the stage of an inverted phase-contrast microscope. The bath buffer consisted of 142 mM NaCl, 1.3 mM KCl, 0.8 m $MgSO_4$, 0.9 mM NaH_2PO_4, 1.8 mM $CaCl_2$, 4.0 mM CsCl, 2.0 mM TEACl, 5.5 mM dextrose and 10 mM HEPES (pH 7.5, adjusted using 1 N NaOH). The pipette solution contained 140 mM KCl, 4.9 mM CsCl, 2.0 mM TEACl 3.0 mM $CaCl_2$, 5.0 mM K_4BAPTA, 1.0 mM $MgCl_2$ and 25 mM HEPES (pH 7.5, adjusted using 1 N KOH). MgATP was added to a final concentration of 3.0 mM before analyses. Junctional currents were recorded using the double whole-cell recording technique by using an EPC 10 USB Double (HEKA Elektronik). Patch electrodes featured a tip resistance of 4-6 MΩ. All experiments were performed at room temperature (25°C). To investigate the polyamine sensitivity of Cx39.4, spermidine (15 or 30 mM) was added into one side of the pipette.

Statistical analysis

Results are presented as mean±s.d. of the number of independent experiments indicated in each figure legend. *P*-values were calculated using Student's *t*-test and a 95% confidence level was considered significant. Statistical analysis was performed using Origin (OriginLab).

Acknowledgements

We thank H. Soma for his technical assistance in the electrophysiological experiments.

Competing interests

The authors declare no competing or financial interests.

Author contributions

Conceptualization: Y.U., M.W.; Methodology: M.W.; Validation: M.W.; Formal analysis: Y.U., S.K., M.W.; Investigation: Y.U., T.A., M.W.; Resources: M.W.; Data curation: M.W.; Writing - original draft: Y.U., M.W.; Writing - review & editing: Y.U., S.K., M.W.; Visualization: M.W.; Supervision: M.W.; Project administration: M.W.; Funding acquisition: Y.U., S.K., M.W.

Funding

This work was supported by the Japan Society for the Promotion of Science (KAKENHI grants 15K0079 and 17H03683 to M.W.), by the Ministry of Education, Culture, Sports, Science, and Technology of Japan (KAKENHI grant 22127003 to S.K.), by the Core Research for Evolutional Science and Technology (CREST) program of the Japan Science and Technology Agency (to S.K.) and by a Japan Society for the Promotion of Science fellowship (19J12372 to Y.U.).

Supplementary information

Supplementary information available online at
http://dev.biologists.org/lookup/doi/10.1242/dev.181065.supplemental

References

Bruzzone, R., White, T. W. and Paul, D. L. (1996). Connections with connexins: the molecular basis of direct intercellular signaling. *Eur. J. Biochem.* **238**, 1-27. doi:10.1111/j.1432-1033.1996.0001q.x

Coleman, C. S., Stanley, B. A., Jones, A. D. and Pegg, A. E. (2004). Spermidine/spermine-N1-acetyltransferase-2 (SSAT2) acetylates thialysine and is not

involved in polyamine metabolism. *Biochem. J.* **384**, 139-148. doi:10.1042/BJ20040790

Dooley, C. M., Mongera, A., Walderich, B. and Nusslein-Volhard, C. (2013). On the embryonic origin of adult melanophores: the role of ErbB and Kit signalling in establishing melanophore stem cells in zebrafish. *Development* **140**, 1003-1013. doi:10.1242/dev.087007

Eastman, S. D., Chen, T. H.-P., Falk, M. M., Mendelson, T. C. and Iovine, M. K. (2006). Phylogenetic analysis of three complete gap junction gene families reveals lineage-specific duplications and highly supported gene classes. *Genomics* **87**, 265-274. doi:10.1016/j.ygeno.2005.10.005

Eom, D. S. and Parichy, D. M. (2017). A macrophage relay for long-distance signaling during postembryonic tissue remodeling. *Science* **355**, 1317-1320. doi:10.1126/science.aal2745

Eom, D. S., Inoue, S., Patterson, L. B., Gordon, T. N., Slingwine, R., Kondo, S., Watanabe, M. and Parichy, D. M. (2012). Melanophore migration and survival during zebrafish adult pigment stripe development require the immunoglobulin superfamily adhesion molecule Igsf11. *PLoS Genet.* **8**, e1002899. doi:10.1371/journal.pgen.1002899

Eom, D. S., Bain, E. J., Patterson, L. B., Grout, M. E. and Parichy, D. M. (2015). Long-distance communication by specialized cellular projections during pigment pattern development and evolution. *Elife* **4**, e12401. doi:10.7554/eLife.12401

Fadeev, A., Krauss, J., Frohnhöfer, H. G., Irion, U. and Nusslein-Volhard, C. (2015). Tight Junction Protein 1a regulates pigment cell organisation during zebrafish colour patterning. *Elife* **4**, e06545. doi:10.7554/eLife.06545

Fadeev, A., Krauss, J., Singh, A. P. and Nusslein-Volhard, C. (2016). Zebrafish Leucocyte tyrosine kinase controls iridophore establishment, proliferation and survival. *Pigment Cell Melanoma Res.* **29**, 284-296. doi:10.1111/pcmr.12454

Fadeev, A., Mendoza-Garcia, P., Irion, U., Guan, J., Pfeifer, K., Wiessner, S., Serluca, F., Singh, A. P., Nusslein-Volhard, C. and Palmer, R. H. (2018). ALKALs are in vivo ligands for ALK family receptor tyrosine kinases in the neural crest and derived cells. *Proc. Natl. Acad. Sci. USA* **115**, E630-E638. doi:10.1073/pnas.1719137115

Ferrell, J. E., Jr. and Machleder, E. M. (1998). The biochemical basis of an all-or-none cell fate switch in Xenopus oocytes. *Science* **280**, 895-898. doi:10.1126/science.280.5365.895

Frohnhöfer, H. G., Krauss, J., Maischein, H.-M. and Nusslein-Volhard, C. (2013). Iridophores and their interactions with other chromatophores are required for stripe formation in zebrafish. *Development* **140**, 2997-3007. doi:10.1242/dev.096719

Frohnhöfer, H. G., Geiger-Rudolph, S., Pattky, M., Meixner, M., Huhn, C., Maischein, H.-M., Geisler, R., Gehring, I., Maderspacher, F., Nusslein-Volhard, C. et al. (2016). Spermidine, but not spermine, is essential for pigment pattern formation in zebrafish. *Biol. Open* **5**, 736-744. doi:10.1242/bio.018721

Fujioka, A., Terai, K., Itoh, R. E., Aoki, K., Nakamura, T., Kuroda, S., Nishida, E. and Matsuda, M. (2006). Dynamics of the Ras/ERK MAPK cascade as monitored by fluorescent probes. *J. Biol. Chem.* **281**, 8917-8926. doi:10.1074/jbc.M509344200

Giepmans, B. N., Verlaan, I. and Moolenaar, W. H. (2001). Connexin-43 interactions with ZO-1 and alpha- and beta-tubulin. *Cell Commun. Adhes.* **8**, 219-223. doi:10.3109/15419060109080727

Gonzalez, D., Gomez-Hernandez, J. M. and Barrio, L. C. (2007). Molecular basis of voltage dependence of connexin channels: an integrative appraisal. *Prog. Biophys. Mol. Biol.* **94**, 66-106. doi:10.1016/j.pbiomolbio.2007.03.007

Hamada, H., Watanabe, M., Lau, H. E., Nishida, T., Hasegawa, T., Parichy, D. M. and Kondo, S. (2014). Involvement of Delta/Notch signaling in zebrafish adult pigment stripe patterning. *Development* **141**, 318-324. doi:10.1242/dev.099804

Hirata, M., Nakamura, K., Kanemaru, T., Shibata, Y. and Kondo, S. (2003). Pigment cell organization in the hypodermis of zebrafish. *Dev. Dyn.* **227**, 497-503. doi:10.1002/dvdy.10334

Hirata, M., Nakamura, K. and Kondo, S. (2005). Pigment cell distributions in different tissues of the zebrafish, with special reference to the striped pigment pattern. *Dev. Dyn.* **234**, 293-300. doi:10.1002/dvdy.20513

Hoptak-Solga, A. D., Klein, K. A., DeRosa, A. M., White, T. W. and Iovine, M. K. (2007). Zebrafish short fin mutations in connexin43 lead to aberrant gap junctional intercellular communication. *FEBS Lett.* **581**, 3297-3302. doi:10.1016/j.febslet.2007.06.030

Inaba, M., Yamanaka, H. and Kondo, S. (2012). Pigment pattern formation by contact-dependent depolarization. *Science* **335**, 677. doi:10.1126/science.1212821

Inoue, S., Kondo, S., Parichy, D. M. and Watanabe, M. (2014). Tetraspanin 3c requirement for pigment cell interactions and boundary formation in zebrafish adult pigment stripes. *Pigment Cell Melanoma Res.* **27**, 190-200. doi:10.1111/pcmr.12192

Irion, U., Frohnhöfer, H. G., Krauss, J., Colak Champollion, T., Maischein, H. M., Geiger-Rudolph, S., Weiler, C. and Nusslein-Volhard, C. (2014). Gap junctions composed of connexins 41.8 and 39.4 are essential for colour pattern formation in zebrafish. *Elife* **3**, e05125. doi:10.7554/eLife.05125

Iwashita, M., Watanabe, M., Ishii, M., Chen, T., Johnson, S. L., Kurachi, Y., Okada, N. and Kondo, S. (2006). Pigment pattern in jaguar/obelix zebrafish is caused by a Kir7.1 mutation: implications for the regulation of melanosome movement. *PLoS Genet.* **2**, e197. doi:10.1371/journal.pgen.0020197

Kawakami, K., Koga, A., Hori, H. and Shima, A. (1998). Excision of the tol2 transposable element of the medaka fish, Oryzias latipes, in zebrafish, Danio rerio. *Gene* **225**, 17-22. doi:10.1016/S0378-1119(98)00537-X

Kawakami, K., Shima, A. and Kawakami, N. (2000). Identification of a functional transposase of the Tol2 element, an Ac-like element from the Japanese medaka fish, and its transposition in the zebrafish germ lineage. *Proc. Natl. Acad. Sci. USA* **97**, 11403-11408. doi:10.1073/pnas.97.21.11403

Klaassen, L. J., de Graaff, W., van Asselt, J. B., Klooster, J. and Kamermans, M. (2016). Specific connectivity between photoreceptors and horizontal cells in the zebrafish retina. *J. Neurophysiol.* **116**, 2799-2814. doi:10.1152/jn.00449.2016

Kondo, S. and Asai, R. (1995). A reaction-diffusion wave on the skin of the marine angelfish Pomacanthus. *Nature* **376**, 765-768. doi:10.1038/376765a0

Kosakovsky Pond, S. L., Mannino, F. V., Gravenor, M. B., Muse, S. V. and Frost, S. D. (2007). Evolutionary model selection with a genetic algorithm: a case study using stem RNA. *Mol. Biol. Evol.* **24**, 159-170. doi:10.1093/molbev/msl144

Krauss, J., Astrinidis, P., Astrinides, P., Frohnhöfer, H. G., Walderich, B. and Nusslein-Volhard, C. (2013). transparent, a gene affecting stripe formation in Zebrafish, encodes the mitochondrial protein Mpv17 that is required for iridophore survival. *Biol. Open* **2**, 703-710. doi:10.1242/bio.20135132

Kumar, N. M. and Gilula, N. B. (1996). The gap junction communication channel. *Cell* **84**, 381-388. doi:10.1016/S0092-8674(00)81282-9

Kumari, S. S., Varadaraj, K., Valiunas, V., Ramanan, S. V., Christensen, E. A., Beyer, E. C. and Brink, P. R. (2000). Functional expression and biophysical properties of polymorphic variants of the human gap junction protein connexin37. *Biochem. Biophys. Res. Commun.* **274**, 216-224. doi:10.1006/bbrc.2000.3054

Lang, M. R., Patterson, L. B., Gordon, T. N., Johnson, S. L. and Parichy, D. M. (2009). Basonuclin-2 requirements for zebrafish adult pigment pattern development and female fertility. *PLoS Genet.* **5**, e1000744. doi:10.1371/journal.pgen.1000744

Levin, M. (2007). Gap junctional communication in morphogenesis. *Prog. Biophys. Mol. Biol.* **94**, 186-206. doi:10.1016/j.pbiomolbio.2007.03.005

Levin, M. and Mercola, M. (1999). Gap junction-mediated transfer of left-right patterning signals in the early chick blastoderm is upstream of Shh asymmetry in the node. *Development* **126**, 4703-4714.

Lien, Y.-C., Ou, T.-Y., Lin, Y.-T., Kuo, P.-C. and Lin, H.-J. (2013). Duplication and diversification of the spermidine/spermine N1-acetyltransferase 1 genes in zebrafish. *PLoS ONE* **8**, e54017. doi:10.1371/journal.pone.0054017

Lin, X., Fenn, E. and Veenstra, R. D. (2006). An amino-terminal lysine residue of rat connexin40 that is required for spermine block. *J. Physiol.* **570**, 251-269. doi:10.1113/jphysiol.2005.097188

Lister, J. A., Robertson, C. P., Lepage, T., Johnson, S. L. and Raible, D. W. (1999). nacre encodes a zebrafish microphthalmia-related protein that regulates neural-crest-derived pigment cell fate. *Development* **126**, 3757-3767.

Liu, T. A., Chang, H. K. and Shieh, R. C. (2012). Revisiting inward rectification: K ions permeate through Kir2.1 channels during high-affinity block by spermidine. *J. Gen. Physiol.* **139**, 245-259. doi:10.1085/jgp.201110736

Maderspacher, F. and Nusslein-Volhard, C. (2003). Formation of the adult pigment pattern in zebrafish requires leopard and obelix dependent cell interactions. *Development* **130**, 3447-3457. doi:10.1242/dev.00519

Mahalwar, P., Walderich, B., Singh, A. P. and Nusslein-Volhard, C. (2014). Local reorganization of xanthophores fine-tunes and colors the striped pattern of zebrafish. *Science* **345**, 1362-1364. doi:10.1126/science.1254837

Mahalwar, P., Singh, A. P., Fadeev, A., Nusslein-Volhard, C. and Irion, U. (2016). Heterotypic interactions regulate cell shape and density during color pattern formation in zebrafish. *Biol. Open* **5**, 1680-1690. doi:10.1242/bio.022251

Mathews, J. and Levin, M. (2017). Gap junctional signaling in pattern regulation: Physiological network connectivity instructs growth and form. *Dev. Neurobiol.* **77**, 643-673. doi:10.1002/dneu.22405

Meinhardt, H. (1995). *The Algorithmic Beauty of Sea Shells*. Berlin & Heidelberg: Springer-Verlag.

Meinhardt, H. and Gierer, A. (1974). Applications of a theory of biological pattern formation based on lateral inhibition. *J. Cell Sci.* **15**, 321-346.

Meinhardt, H. and Gierer, A. (2000). Pattern formation by local self-activation and lateral inhibition. *BioEssays* **22**, 753-760. doi:10.1002/1521-1878(200008)22:8<753::AID-BIES9>3.0.CO;2-Z

Milos, N., Dingle, A. D. and Milos, J. P. (1983). Dynamics of pigment pattern formation in the zebrafish, Brachydanio rerio. III. Effect of anteroposterior location of three-day lateral line melanophores on colonization by the second wave of melanophores. *J. Exp. Zool.* **227**, 81-92. doi:10.1002/jez.1402270112

Misu, A., Yamanaka, H., Aramaki, T., Kondo, S., Skerrett, I. M., Iovine, M. K. and Watanabe, M. (2016). Two different functions of connexin43 confer two different bone phenotypes in zebrafish. *J. Biol. Chem.* **291**, 12601-12611. doi:10.1074/jbc.M116.720110

Miyamoto, S., Kashiwagi, K., Ito, K., Watanabe, S. and Igarashi, K. (1993). Estimation of polyamine distribution and polyamine stimulation of protein synthesis in Escherichia coli. *Arch. Biochem. Biophys.* **300**, 63-68. doi:10.1006/abbi.1993.1009

Musa, H. and Veenstra, R. D. (2003). Voltage-dependent blockade of connexin40 gap junctions by spermine. *Biophys. J.* **84**, 205-219. doi:10.1016/S0006-3495(03)74843-7
Musa, H., Fenn, E., Crye, M., Gemel, J., Beyer, E. C. and Veenstra, R. D. (2004). Amino terminal glutamate residues confer spermine sensitivity and affect voltage gating and channel conductance of rat connexin40 gap junctions. *J. Physiol.* **557**, 863-878. doi:10.1113/jphysiol.2003.059386
Nakamasu, A., Takahashi, G., Kanbe, A. and Kondo, S. (2009). Interactions between zebrafish pigment cells responsible for the generation of Turing patterns. *Proc. Natl. Acad. Sci. USA* **106**, 8429-8434. doi:10.1073/pnas.0808622106
Odenthal, J., Rossnagel, K., Haffter, P., Kelsh, R. N., Vogelsang, E., Brand, M., van Eeden, F. J., Furutani-Seiki, M., Granato, M., Hammerschmidt, M. et al. (1996). Mutations affecting xanthophore pigmentation in the zebrafish, Danio rerio. *Development* **123**, 391-398. doi:10.1016/0736-5748(96)80313-3
Parichy, D. M. and Turner, J. M. (2003). Temporal and cellular requirements for Fms signaling during zebrafish adult pigment pattern development. *Development* **130**, 817-833. doi:10.1242/dev.00307
Parichy, D. M., Ransom, D. G., Paw, B., Zon, L. I. and Johnson, S. L. (2000). An orthologue of the kit-related gene fms is required for development of neural crest-derived xanthophores and a subpopulation of adult melanocytes in the zebrafish, Danio rerio. *Development* **127**, 3031-3044.
Patterson, L. B. and Parichy, D. M. (2013). Interactions with iridophores and the tissue environment required for patterning melanophores and xanthophores during zebrafish adult pigment stripe formation. *PLoS Genet.* **9**, e1003561. doi:10.1371/journal.pgen.1003561
Plotkin, L. I., Laird, D. W. and Amedee, J. (2016). Role of connexins and pannexins during ontogeny, regeneration, and pathologies of bone. *BMC Cell Biol.* **17** Suppl. 1, 19. doi:10.1186/s12860-016-0088-6
Prum, R. O. and Williamson, S. (2002). Reaction-diffusion models of within-feather pigmentation patterning. *Proc. Biol. Sci.* **269**, 781-792. doi:10.1098/rspb.2001.1896
Saez, J. C., Berthoud, V. M., Branes, M. C., Martinez, A. D. and Beyer, E. C. (2003). Plasma membrane channels formed by connexins: their regulation and functions. *Physiol. Rev.* **83**, 1359-1400. doi:10.1152/physrev.00007.2003
Saunders, L. M., Mishra, A. K., Aman, A. J., Lewis, V. M., Toomey, M. B., Packer, J. S., Qiu, X., McFaline-Figueroa, J. L., Corbo, J. C., Trapnell, C. et al. (2019). Thyroid hormone regulates distinct paths to maturation in pigment cell lineages. *Elife* **8**, e45181. doi:10.7554/eLife.45181
Sawada, R., Aramaki, T. and Kondo, S. (2018). Flexibility of pigment cell behavior permits the robustness of skin pattern formation. *Genes Cells* **23**, 537-545. doi:10.1111/gtc.12596
Simpson, I., Rose, B. and Loewenstein, W. R. (1977). Size limit of molecules permeating the junctional membrane channels. *Science* **195**, 294-296. doi:10.1126/science.831276
Singh, A. P., Schach, U. and Nusslein-Volhard, C. (2014). Proliferation, dispersal and patterned aggregation of iridophores in the skin prefigure striped colouration of zebrafish. *Nat. Cell Biol.* **16**, 607-614. doi:10.1038/ncb2955
Singh, A. P., Frohnhöfer, H. G., Irion, U. and Nusslein-Volhard, C. (2015). Fish pigmentation. Response to Comment on “Local reorganization of xanthophores fine-tunes and colors the striped pattern of zebrafish”. *Science* **348**, 297. doi:10.1126/science.aaa2804
Smyth, J. W., Vogan, J. M., Buch, P. J., Zhang, S.-S., Fong, T. S., Hong, T.-T. and Shaw, R. M. (2012). Actin cytoskeleton rest stops regulate anterograde traffic of connexin 43 vesicles to the plasma membrane. *Circ. Res.* **110**, 978-989. doi:10.1161/CIRCRESAHA.111.257964
Suchyna, T. M., Nitsche, J. M., Chilton, M., Harris, A. L., Veenstra, R. D. and Nicholson, B. J. (1999). Different ionic selectivities for connexins 26 and 32 produce rectifying gap junction channels. *Biophys. J.* **77**, 2968-2987. doi:10.1016/S0006-3495(99)77129-8
Takahashi, G. and Kondo, S. (2008). Melanophores in the stripes of adult zebrafish do not have the nature to gather, but disperse when they have the space to move. *Pigment Cell Melanoma Res* **21**, 677-686. doi:10.1111/j.1755-148X.2008.00504.x
Theis, M., Söhl, G., Eiberger, J. and Willecke, K. (2005). Emerging complexities in identity and function of glial connexins. *Trends Neurosci.* **28**, 188-195. doi:10.1016/j.tins.2005.02.006
Toyofuku, T., Yabuki, M., Otsu, K., Kuzuya, T., Hori, M. and Tada, M. (1998). Direct association of the gap junction protein connexin-43 with ZO-1 in cardiac myocytes. *J. Biol. Chem.* **273**, 12725-12731. doi:10.1074/jbc.273.21.12725
Turing, A. M. (1952). The chemical basis of morphogenesis. *Philos. Trans. R. Soc. Lond. B Biol. Sci.* **237**, 37-72. doi:10.1098/rstb.1952.0012
Unger, V. M., Kumar, N. M., Gilula, N. B. and Yeager, M. (1999). Three-dimensional structure of a recombinant gap junction membrane channel. *Science* **283**, 1176-1180. doi:10.1126/science.283.5405.1176
Usui, Y., Kondo, S. and Watanabe, M. (2018). Melanophore multinucleation pathways in zebrafish. *Dev. Growth Differ.* **60**, 454-459. doi:10.1111/dgd.12564
Verselis, V. K., Ginter, C. S. and Bargiello, T. A. (1994). Opposite voltage gating polarities of two closely related connexins. *Nature* **368**, 348-351. doi:10.1038/368348a0
Vogel, N. L., Boeke, M. and Ashburner, B. P. (2006). Spermidine/Spermine N1-Acetyltransferase 2 (SSAT2) functions as a coactivator for NF-kappaB and cooperates with CBP and P/CAF to enhance NF-kappaB-dependent transcription. *Biochim. Biophys. Acta* **1759**, 470-477. doi:10.1016/j.bbaexp.2006.08.005
Volkening, A. and Sandstede, B. (2018). Iridophores as a source of robustness in zebrafish stripes and variability in Danio patterns. *Nat. Commun.* **9**, 3231. doi:10.1038/s41467-018-05629-z
Wang, X. G. and Peracchia, C. (1997). Positive charges of the initial C-terminus domain of Cx32 inhibit gap junction gating sensitivity to CO2. *Biophys. J.* **73**, 798-806. doi:10.1016/S0006-3495(97)78112-8
Watanabe, M. and Kondo, S. (2012). Changing clothes easily: connexin41.8 regulates skin pattern variation. *Pigment Cell Melanoma Res* **25**, 326-330. doi:10.1111/j.1755-148X.2012.00984.x
Watanabe, M. and Kondo, S. (2015a). Fish pigmentation. Comment on “Local reorganization of xanthophores fine-tunes and colors the striped pattern of zebrafish”. *Science* **348**, 297. doi:10.1126/science.1261947
Watanabe, M. and Kondo, S. (2015b). Is pigment patterning in fish skin determined by the Turing mechanism? *Trends Genet.* **31**, 88-96. doi:10.1016/j.tig.2014.11.005
Watanabe, S., Kusama-Eguchi, K., Kobayashi, H. and Igarashi, K. (1991). Estimation of polyamine binding to macromolecules and ATP in bovine lymphocytes and rat liver. *J. Biol. Chem.* **266**, 20803-20809.
Watanabe, M., Iwashita, M., Ishii, M., Kurachi, Y., Kawakami, A., Kondo, S. and Okada, N. (2006). Spot pattern of leopard Danio is caused by mutation in the zebrafish connexin41.8 gene. *EMBO Rep.* **7**, 893-897. doi:10.1038/sj.embor.7400757
Watanabe, M., Watanabe, D. and Kondo, S. (2012). Polyamine sensitivity of gap junctions is required for skin pattern formation in zebrafish. *Sci. Rep.* **2**, 473. doi:10.1038/srep00473
Watanabe, M., Sawada, R., Aramaki, T., Skerrett, I. M. and Kondo, S. (2016). the physiological characterization of Connexin41.8 and Connexin39.4, which are involved in the striped pattern formation of zebrafish. *J. Biol. Chem.* **291**, 1053-1063. doi:10.1074/jbc.M115.673129
Willecke, K., Eiberger, J., Degen, J., Eckardt, D., Romualdi, A., Guldenagel, M., Deutsch, U. and Söhl, G. (2002). Structural and functional diversity of connexin genes in the mouse and human genome. *Biol. Chem.* **383**, 725-737. doi:10.1515/BC.2002.076
Yamaguchi, M., Yoshimoto, E. and Kondo, S. (2007). Pattern regulation in the stripe of zebrafish suggests an underlying dynamic and autonomous mechanism. *Proc. Natl. Acad. Sci. USA* **104**, 4790-4793. doi:10.1073/pnas.0607790104
Yamanaka, H. and Kondo, S. (2014). In vitro analysis suggests that difference in cell movement during direct interaction can generate various pigment patterns in vivo. *Proc. Natl. Acad. Sci. USA* **111**, 1867-1872. doi:10.1073/pnas.1315416111

Table S1

Table S1. Primer sequences used in RT-PCR

Gene	Forward primer sequence	Reverse primer sequence
cx39.4	TCTCAGCGGCAGAAGCTCCTCAC	GCAGATTCCACAGCCGTGCCAAG
cx41.8	TCATCGGTCAACAGAGATAG	CTAGTACCAAGATCCGGAAG
dct	CGAATCAGCCCGCGTTCACG	TATCCCTCCAGTGCATTCCT
aox5	AGGGCATTGGAGAACCCCCAGT	ACACGTTGATGGCCCACGGT
beta-actin	CGGTTTTGCTGGAGATGATG	CGTGCTCAATGGGGTATTTG
cx28.1	CCCGTCCAACTGAAAAGAGC	AAAACGTTTCAGTGGGGCTC
cx28.9	AGCATGGGAGAATGGGGATT	GGGAGATGGGAAAGGTGTGA
cx32.2	GCTGCGATAACCTGTGCTAC	TGCGTCAAGTAGCTACCCAA
cx32.3	GTTTACATGCTCCCGTTCCC	TCTTCCGACATCCCACTCTG
cx34.5	GTTGAGTCCCTGAGCAGTCT	CCGGCTCCAAGGACTAGAAT
cx39.9	TCTTCGTCTCAACCCCAACA	GAAGCCCACCTCAAACAGTG
cx40.8	AAGGACTTATCATAGCACACG	GGTGACTGGAGCGCACTGGGG
cx43	TTGGTGACTGAACTTCAGAG	TTGAAAGCTGACTGCTCGTC
cx44.1	TAGCTGCCTCATCGATCCAG	GGCAGCGTTTCGTCATACAT
cx45.6	ACTCTACGTCGGTTGGGAAG	ACCCAGTAGCGGATATGAGC
cx48.5	CTGGCTGACGGTACTCTTCA	CCATACGAACGATGTGCAGG
cx50.5	CGAGAATGTGTGCTATGATG	GATCCATTGCCTGGCGCTCCT
cx52.6	AATATTCTCAGCAGCCCCGA	TTGAGTGATACGGTTGGCCT
cx52.7	CCTGGATGCAAGAACGTCTG	GCTCTTCCAACCTCCTCAGT
cx52.9	TGGACCAGGCTTGATCTCAG	GACTGCTCATCGTTCCACAC
cx55.5	ATCCGTTACTGGGTTCTGCA	CTATTTTGCGCCGTACCTCC
cx27.5	CTCTGCCCATGCCACTAAC	TTGGGTGTTGCAGATGAAATGC
cx28.6	TTTCTGCGGGCTCACCACCCTC	CACAAACACCACGGATAGCC
cx28.8	ACGAAGTCCTTGAACTCGTC	AACCACAGGAGTGAACATCAG
cx30.3	ATCTGAATCATCGTGTAGCC	GTCTGACTGTTCGTCTCCCC
cx30.9	CGGCCAAACACAGTGGAGTATTGG	AGGATTCGGAAGATGAACACC
cx31.7	GGGTTGCTGAGTATTGCAGG	TTGAATCAACGATGAATTGGG
cx34.4	ACACAATCACTGCGCTCCGAC	AACCATGACTCTGAAAAGGAAGAC
cx35.4	TAATAAGAGACGGGGAACAG	ATAAACCATGACCCTGAACAC
cx43.4	TTGACCGCCTGCGCAGGCACC	TCTCAATCAAGCATGGATCC
cx44.2	AGGGGCTTCACACAACAGCG	TGAAGTTGAAATCTTGTGCC
cx47.1	TGCTGAAGGGCCGCAGGTTTG	TCAAGACCGTCAGCCAGACC
cx52.8	TCTTCATCGGCGGGCAGACCG	ACGTGGAATGGTGCTGGATCTCC
cx34.1	TTGGAGAGGTTGCTGGAGGC	ATTGGGAAGGCTTTATCGTAGC
cx34.8	GGAGAGTGGACCATTTTAGAGCG	TTTGTCGTAGCAGGCCTGG
cx35	CGTCTCCTGGAGGCGGCTGTCC	TGCAAACCATGATGATCTGG
cx36.7	ACGTTTCGAGATGTTACCAGC	AAGACTCTGGAAATTGTCCTGG
cx40.5	GCCAGTCACCCTAGTCGAAT	AAAGGTGATCTCCAGGACGG
cx46.8	GAGTCCAGGAGTGTTTCGCA	TCAGCCGACTACGTTTGCTT
cx23	TTGCTGTCTACGGCAATGAGGC	AAGATGAAACACTGCTCCAGG
cx24	TTCTGCTACAACCAGTTTAGGC	AACCGAACAGACGACTCTGGA
sat1a.1	TACGTCATGAAGGAGTATCGG	ACTAAACTGAACAGCAGGTG
sat1a.2	CCGTTTTATCACTGCGTCGT	TCCACTCGGCCACTATGAAG
sat1b	GAGCATCAGAAAGTCGAAGG	TGCTGCAACGATTCTTCACTG

Primer pairs were designed to amplify fragment approximately 200 bps.

Figure S1

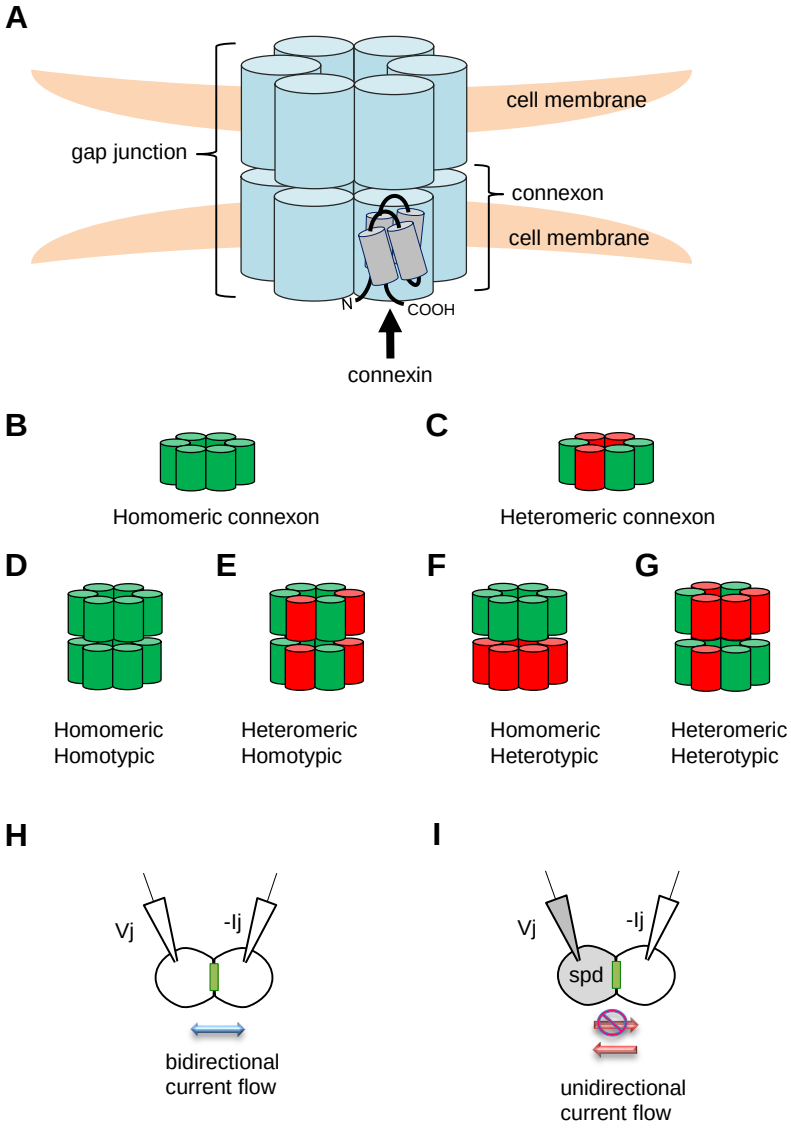

Fig. S1. Schematic representations of gap junction formation and rectification property.
(A) Connexin has four transmembrane domains (gray columns inside of the light blue column), and a cytoplasmic N- and C-terminus. Six connexins oligomerize to form a connexon, and a docking of two connexons on the adjacent cells forms a gap junction. (B) Homomeric connexon is a hexamer which is an assembly of six identical connexins. (C) Heteromeric connexon includes two or more different types of connexins. (D) Homomeric-homotypic gap junction is formed by a docking of identical homomeric-connexons. (E) Heteromeric-homotypic gap junction is formed by a docking of identical heteromeric-connexons. (F) Homomeric-heterotypic gap junction is formed by a docking of different types of homomeric-connexons. and (G) Heteromeric-heterotypic gap junction is formed by a docking of different types of heteromeric-connexons. (H) Homomeric-homotypic gap junction (green box) usually shows bidirectional current flow. (I) Spermidine (spd) injected into one side of cells sometimes blocks the outward flow and causes a rectification property of gap junction.

Figure S2

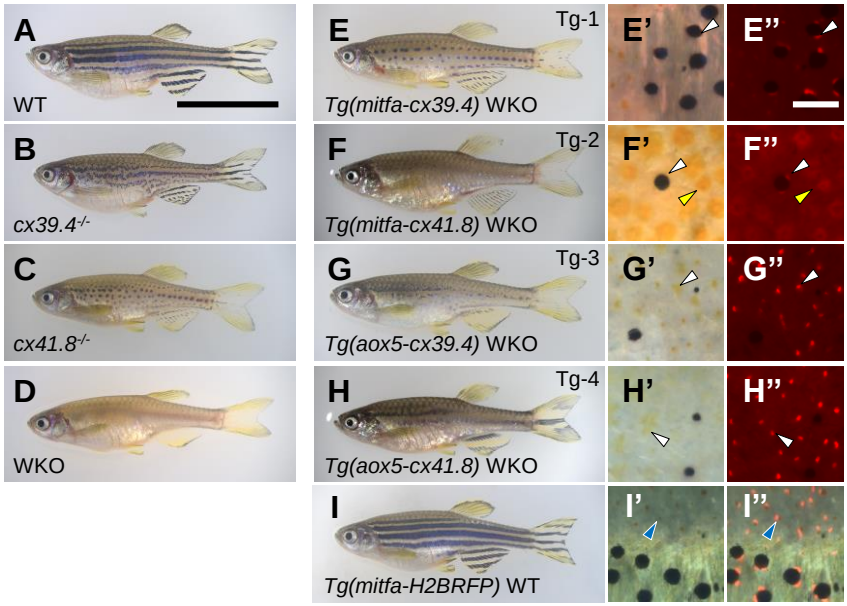

Fig. S2. Representative skin phenotypes of fish. Wild-type (A; WT), *cx39.4*$^{-/-}$ (B; *luchs*), *cx41.8*$^{-/-}$ (C; *leopard*), and double-knockout mutant (D; WKO). (E-I) Transgenic fish lines. Specificities of gene expression in each pigment cell were monitored using a fluorescent reporter protein, H2BRFP (E'-I' and E"-I": magnified images of trunk region in E-I; white arrowheads: cell nuclei; yellow arrowhead: xanthophore autofluorescence signal (F"); blue arrowhead: leaky expression of H2BRFP (I"). Scale bars: 10 mm (A) and 100 μm (E").

Figure S3A

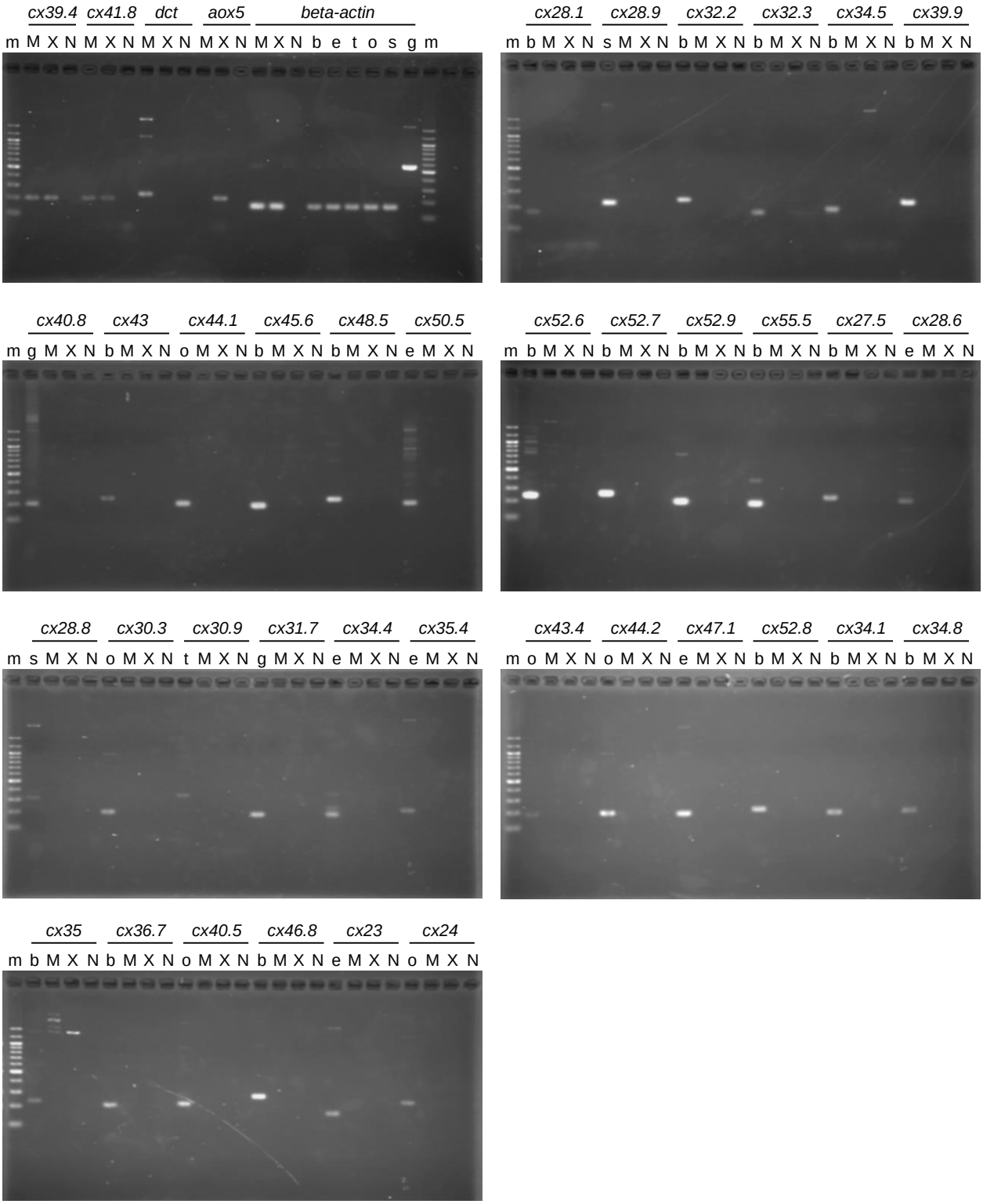

Figure S3B

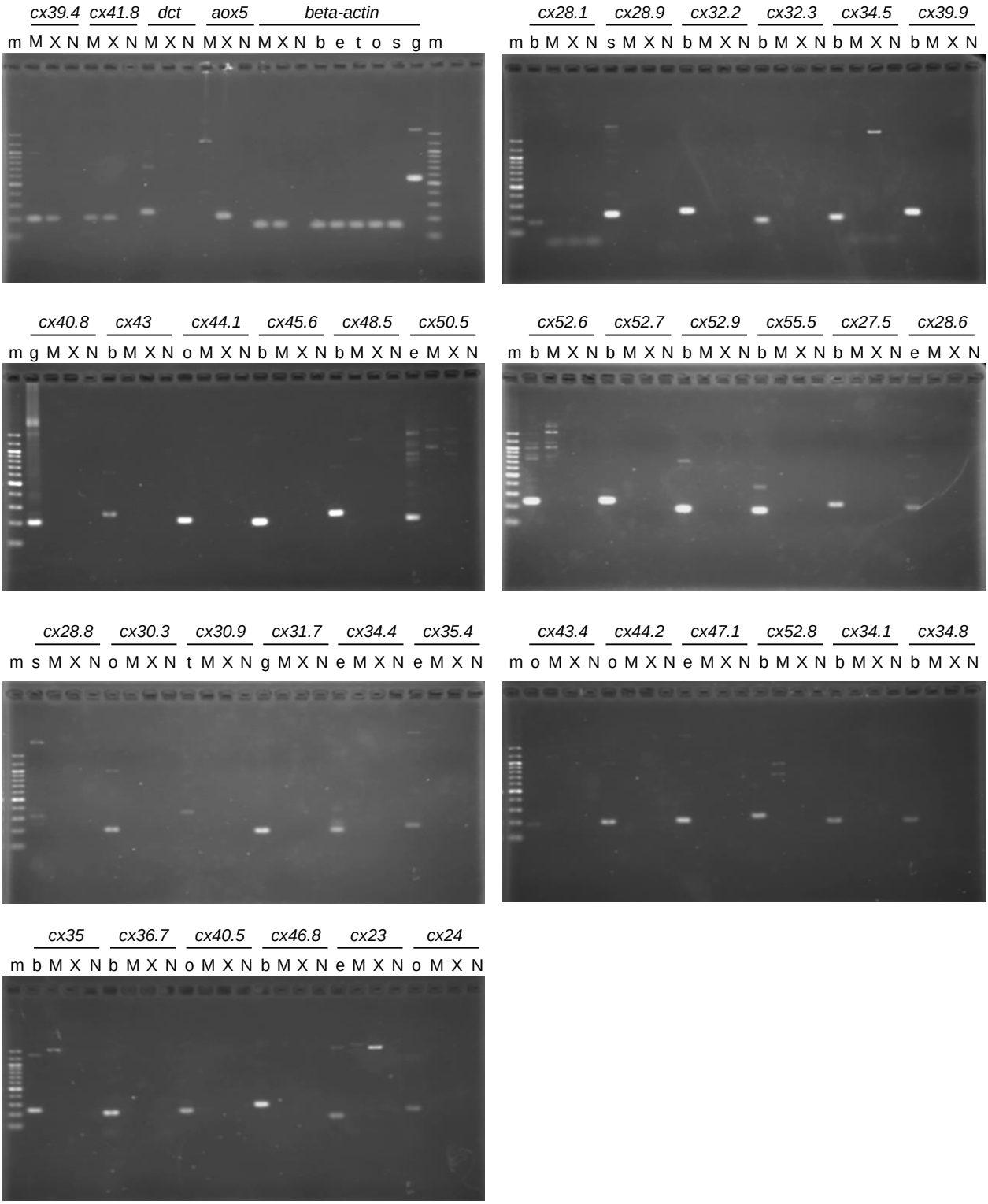

Fig. S3. Connexin expression in melanophores and xanthophores. Gene expression of zebrafish 38 connexin genes in melanophores and xanthophores from trunk (A) and fin (B) were analyzed by RT-PCR. Abbreviations; m, molecular marker; M, melanophore; X, xanthophore; N, negative control (without cDNA). “g”, “b”, “e”, “t”, “o” and “s” are positive controls to check the specificity of primer sets (Table S1); “g”: genomic DNA; “b”, “e”, “t”, “o” and “s”: cDNAs prepared using mRNAs derived from brain, eye, testis, ovary, and skin tissues, respectively. *dct* and *aox5* were positive controls for melanophore- and xanthophore-specific expression, and *beta-actin* was a positive control for RT-PCR. Two independent experiments were performed and the same result was obtained.

Figure S4

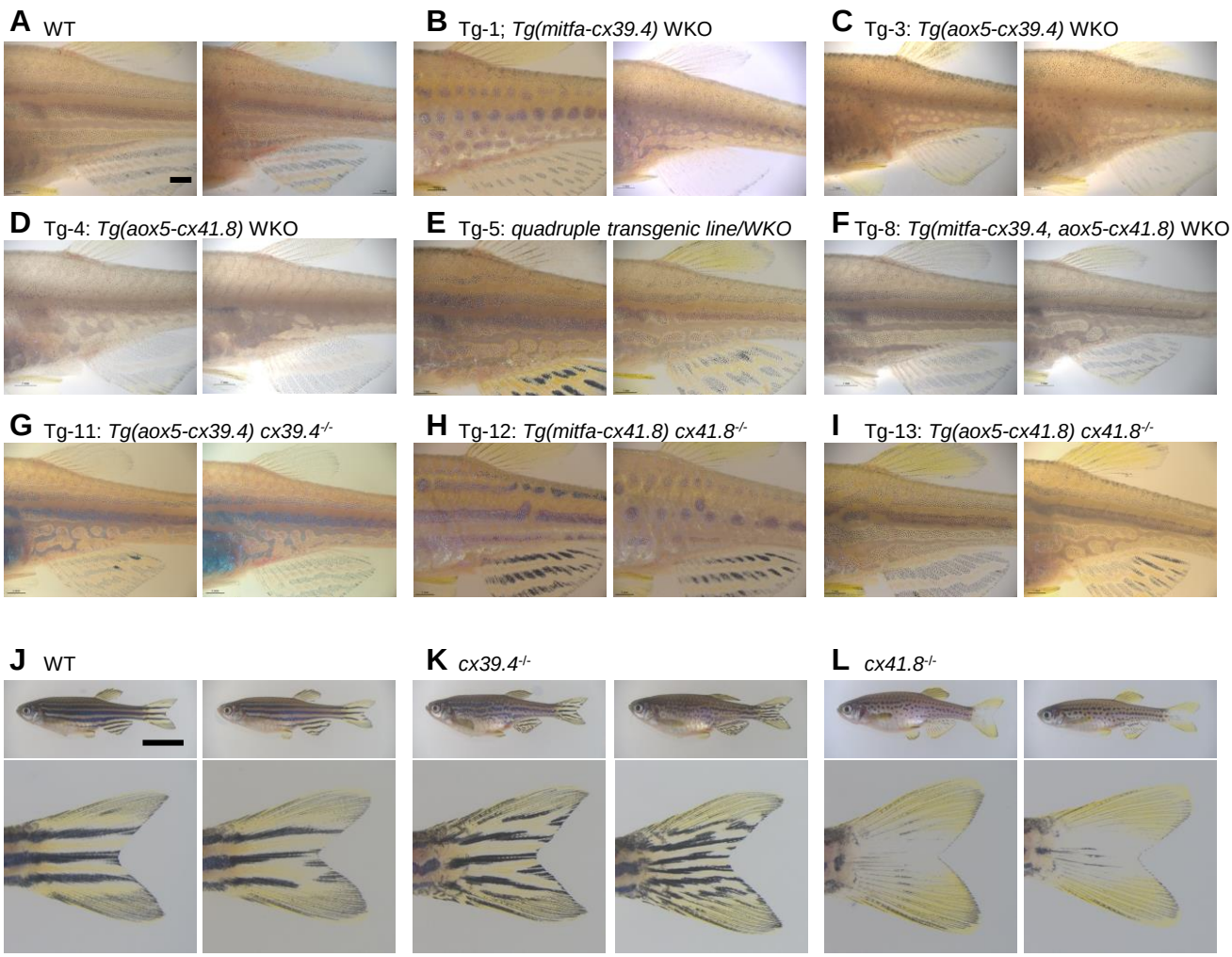

Fig. S4. Skin pattern variation. In each panel, fish pictures represent the thicker/larger pattern on left column and the thinner/smaller pattern on right column, which was what were used for the statistical analysis in Fig. 3. The typical fish phenotypes showing almost the average are shown in Fig. 2. WT (A), Tg-1; *Tg(mitfa-cx39.4)*WKO (B), Tg-3: *Tg(aox5-cx39.4)*WKO (C), Tg-4: *Tg(aox5-cx41.8)*WKO (D), Tg-5: *quadruple transgenic line/WKO* (E), Tg-8: *Tg(mitfa-cx39.4, aox5-cx41.8)*WKO (F), Tg-11: *Tg(aox5-cx39.4) cx39.4*$^{-/-}$ (G), Tg-12: *Tg(mitfa-cx41.8)cx41.8*$^{-/-}$ (H), and Tg-13: *Tg(aox5-cx41.8)cx41.8*$^{-/-}$ (I). (J-K) Fish pictures representing pattern variations on the caudal fin of wild type and mutants. Scale bars: 1 mm in (A) and 10 mm in (J).

Figure S5

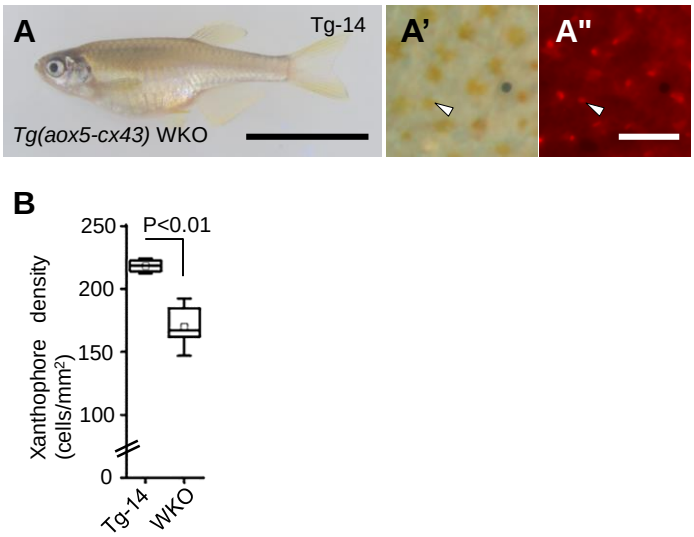

Fig. S5. Cx43 expression in xanthophores increases xanthophore density. (A) A transgenic WKO zebrafish in which *cx43* was expressed in xanthophores. (A', A") Magnified image of skin. Specificity of gene expression in xanthophore was monitored using a fluorescent reporter protein, H2BRFP (white arrowheads). (B) Xanthophore density was examined in Tg-14 line; 2 transgenic fish were used for the density calculation. Tg-14: 218.35 ± 6.01 cells/mm^2; *P*-value (Student's *t*-test) is shown in the graph; error bars: s.d. Intermediate lines in each box are median values and small squares are means. The box width encompasses the first and third quartiles and whiskers show the mean ± s.d. Scale bars: 10 mm (A) and 100 μm (A").

Figure S6

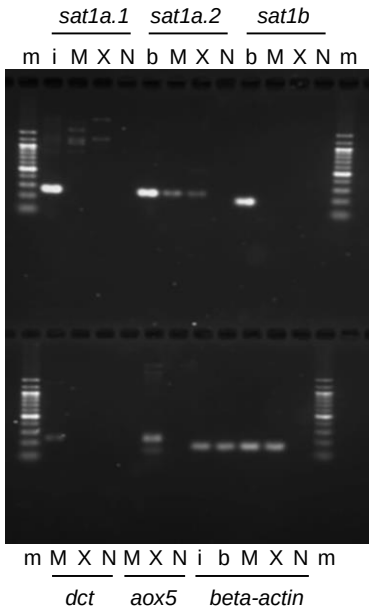

Fig. S6. Gene expression of *ssat1* homologs in melanophores and xanthophores. Gene expressions of three *ssat1* homologs, *sat1a.1*, *sat1a.2*, and *sat1b*, in melanophores and xanthophores from a fish trunk were analyzed by RT-PCR. Abbreviations; M, melanophore; X, xanthophore; N, negative control (without cDNA); m, molecular marker; i, intestine; b, brain. *Dct* and *aox5*, positive controls for melanophore- and xanthophore-specific expression; *beta-actin*: positive control for RT-PCR. Two independent experiments were performed and the same result was obtained.